



**CHALMERS**  
UNIVERSITY OF TECHNOLOGY

---



# **Lateral Control of Heavy Duty Vehicles in Platooning using Model Predictive Control**

Master's thesis in Systems, Control and Mechatronics

**WOLGAN DOVLAND HERRERA**

**NIKLAS LIDANDER**



MASTER'S THESIS 2016:EX-038

# Lateral Control of Heavy Duty Vehicles in Platooning using Model Predictive Control

WOLGAN DOVLAND HERRERA  
NIKLAS LIDANDER



**CHALMERS**  
UNIVERSITY OF TECHNOLOGY

Department of Signals and Systems  
CHALMERS UNIVERSITY OF TECHNOLOGY  
Gothenburg, Sweden 2016

Lateral Control of Heavy Duty Vehicles in Platooning using Model Predictive Control

WOLGAN DOVLAND HERRERA  
NIKLAS LIDANDER

© WOLGAN DOVLAND HERRERA & NIKLAS LIDANDER, 2016.

Supervisor: Erik Nordin, Volvo Group Trucks Technology  
Supervisor & Examiner: Nikolce Murgovski, Department of Signals and Systems,  
Chalmers University of Technology

Master's Thesis 2016:EX-038  
Department of Signals and Systems  
Chalmers University of Technology  
SE-412 96 Gothenburg  
Telephone +46 31 772 1000

Typeset in L<sup>A</sup>T<sub>E</sub>X  
Gothenburg, Sweden 2016

Lateral Control of Heavy Duty Vehicles in Platooning using Model Predictive Control

WOLGAN DOVLAND HERRERA  
NIKLAS LIDANDER

Department of Signals and Systems  
Chalmers University of Technology

## Abstract

Fuel cost for transportation of heavy duty vehicles (HDVs) is a considerable portion of the total operational cost. Small reductions of fuel consumption yield substantial savings both economically and environmentally. In recent years, with increasing environmental concern and the desire to reduce greenhouse gases, Intelligent Transportation Systems, like platooning, has gained increased attention for companies and researchers. A vehicle platoon is a convoy of vehicles driving at close inter-vehicular distance in order to reduce air drag, thus saving fuel and increasing traffic efficiency.

Driving at close distances has safety issues since the field of view of a human driver is then limited, which makes it difficult to adapt to changes in the road curvature. Thus, safe driving with short inter-vehicular distances requires automatic control in both the longitudinal and lateral direction. This thesis focuses on the lateral control of HDVs in platooning. A review of previous research was performed and Model Predictive Control (MPC) was chosen as control strategy. An MPC is designed, implemented and evaluated in the Simulink based simulation environment PreScan using high-fidelity HDV models provided by Volvo Group Trucks Technology (Volvo GTT).

The results show that the platoon is able to avoid string instability by tracking the leading vehicle. Furthermore, the platoon is able to avoid obstacles within its lane and tracks the leading vehicle with maximum deviation of 10 cm without sensor noise. The developed MPC can be used as a regular lane keeping system by tracking the middle of the road instead of a leading vehicle. Additionally, a Kalman filter is implemented and evaluated in presence of noise. Given the performance of the MPC and its lane keeping capabilities, MPC seems to be a suitable choice for platooning, especially since its main drawback, the computational demand, is a diminishing problem as technology advances.

Keywords: Model predictive control, platooning, heavy duty vehicles, lateral control, autonomous vehicles, active safety.



Lateral Control of Heavy Duty Vehicles in Platooning using Model Predictive Control

WOLGAN DOVLAND HERRERA

NIKLAS LIDANDER

Department of Signals and Systems

Chalmers University of Technology

## Sammanfattning

Bränslekostnaden för transporter av tunga fordon är en betydande del av den totala operationskostnaden. Små minskningar av bränsleförbrukning leder till substantiella insparningar, både ekonomiskt och miljömässigt. I och med ökat miljötänkande och kraven på att minska utsläppen av växthusgaser har 'Intelligent Transportation Systems', exempelvis platooning, fått ökat intresse och uppmärksamhet från både företag och forskare. En fordonsplatoon är en konvoj av fordon som kör med små avstånd mellan fordonen vilket leder till minskat luftmotstånd och därmed besparing av bränsle samt ökad trafikeffektivitet.

Att köra med små avstånd mellan fordonen medför säkerhetsrisker eftersom synfältet för en mänsklig förare då är begränsat, vilket gör det svårt att anpassa sig till förändringar av vägens kurvatur. Således kräver säker körning med små avstånd mellan fordonen automatisk reglering både longitudinellt och lateralt. Denna tesen fokuserar på den laterala kontrolleringen av tunga fordon i platooning. En genomgång av tidigare forskning genomfördes vilket medförde att Modellprediktiv Reglering (MPC) valdes som kontrollstrategi. I denna tes är därmed en MPC designad, implementerad och utvärderad i den Simulink-baserade simulationsmiljön PreScan. För valideringen av platoonen användes noggranna fordonsmodeller av tunga fordon tillhandahållna av Volvo Group Trucks Technology (Volvo GTT).

Resultaten visar att platoonen klarar av att undvika string-instabilitet genom att följa ledarfordonet. Vidare är platoonen kapabel till att undvika objekt inom filen den kör i och följer även ledarfordonet med ett maximalt fel på 10 cm utan sensorbrus. Den framtagna MPC:n kan även användas till vanlig filföljning (lane keeping) genom att följa mitten av filen istället för ledarfordonet. Ett Kalmanfilter har även utvecklats som har implementerats och validerats när brus och mätbortfall varit närvarande. Givet MPC:ns prestanda och hur den håller fordonen i filen, verkar MPC vara ett passande val för platooning. Speciellt eftersom MPCs största nackdel, den höga beräkningsbördan, är ett problem som minskar allteftersom teknologin utvecklas.

Nyckelord: Modellprediktiv reglering, platooning, tunga fordon, lateralreglering, autonoma fordon, aktiv säkerhet.



## Acknowledgements

We would like to express our gratitude to Volvo Group Trucks Technology (Volvo GTT) at Advanced Technology & Research for giving us the opportunity to do our master's thesis at Volvo. Specifically we would like to thank our supervisor Erik Nordin and co-supervisor Susanna Leanderson Olsson at Volvo GTT for the continuous support throughout the thesis. Furthermore, we would also like to thank the rest of the group at Vehicle Dynamics and Active Safety, especially Mansour Keshavarz, Vivetha Natterjee, Shant Abraham, Petter Wirfält for providing support when needed. From the Human Factors group we would like to thank Anders K Holmström for help with the simulation environment.

Lastly, our biggest thanks go to our supervisor and examiner Nikolce Murgovski for his support, encouragement and guidance from beginning to end.

Wolgan Dovland Herrera, Niklas Lidander, Gothenburg, June 2016



# Contents

<b>1</b>	<b>Introduction</b>	<b>1</b>
1.1	Background . . . . .	1
1.2	Problem formulation and objectives . . . . .	2
1.3	Scope and limitations . . . . .	3
1.4	Choice of control strategy . . . . .	3
1.4.1	MPC methods in platooning . . . . .	4
1.5	Thesis outline . . . . .	4
<b>2</b>	<b>Theoretical background</b>	<b>5</b>
2.1	Model Predictive Control . . . . .	5
2.2	Smooth Control . . . . .	7
2.2.1	Limiting changes of $u(k)$ . . . . .	7
2.2.2	Limiting changes of $\Delta u(k)$ . . . . .	7
2.3	Constraint management . . . . .	8
2.4	Utilizing preview information . . . . .	8
2.5	Kalman filter . . . . .	9
<b>3</b>	<b>System Description</b>	<b>11</b>
3.1	Platoon setup . . . . .	11
3.2	Reference generation . . . . .	12
3.2.1	Reference generation based on preceding vehicle . . . . .	13
3.2.2	Reference generation based on leading vehicle . . . . .	14
3.3	Modelling . . . . .	16
3.3.1	Lateral vehicle dynamics . . . . .	16
3.3.2	Lateral position dynamics . . . . .	18
3.3.3	Discretization . . . . .	20
3.3.4	Discrete model . . . . .	21
3.4	Sensors . . . . .	22
3.4.1	Camera . . . . .	22
3.4.2	Radar . . . . .	22
3.4.3	Internal vehicle states . . . . .	22
3.4.4	V2V . . . . .	22
<b>4</b>	<b>Implementation</b>	<b>23</b>
4.1	MPC formulation . . . . .	23
4.1.1	FORCES Pro . . . . .	24

4.2	MPC formulation in standard form . . . . .	24
4.3	Kalman filters . . . . .	26
4.4	Modelling losses of lane marking detection . . . . .	27
4.5	Simulation . . . . .	28
4.5.1	Computer hardware specifications . . . . .	28
4.5.2	PreScan . . . . .	28
4.5.3	Structure of implemented components and signal routing . . .	30
<b>5</b>	<b>Results</b>	<b>31</b>
5.1	Lateral control performance . . . . .	32
5.1.1	Reference tracking using preceding vehicle approach . . . . .	32
5.1.1.1	Curve . . . . .	33
5.1.1.2	Obstacle avoidance . . . . .	34
5.1.2	Reference tracking using leading vehicle approach . . . . .	34
5.1.2.1	Curve . . . . .	35
5.1.2.2	Obstacle avoidance . . . . .	36
5.2	Ride comfort with and without preview information . . . . .	37
5.2.1	Curve . . . . .	37
5.2.2	Obstacle avoidance . . . . .	38
5.3	Safety . . . . .	39
5.4	Kalman filter performance . . . . .	40
5.5	Lateral control performance with added noise . . . . .	41
5.6	Lateral control performance with added noise and sensor failures . . .	43
5.7	Computation time . . . . .	45
<b>6</b>	<b>Discussion</b>	<b>47</b>
<b>7</b>	<b>Conclusion</b>	<b>51</b>
<b>8</b>	<b>Future Work</b>	<b>53</b>

# 1

## Introduction

Heavy duty vehicles (HDVs) transport 18 billion tonnes per year in Europe, which is 75% of Europe's total land-transportation of goods [1]. It follows that large amounts of fuel are used, and that even small reductions of fuel consumption, which are 25-30% of a HDVs operating cost [2], yields substantial savings, both economically and environmentally. The increased environmental concern together with the desire to reduce greenhouse gas emissions have made Intelligent Transportation Systems gain increased attention to face the future challenges in the transport sector.

### 1.1 Background

Volvo Group Trucks Technology (Volvo GTT) is at the frontier of the highly competitive transport business, and thus interested in reducing fuel usage. Platooning of HDVs is one way of reducing the fuel consumption and increasing traffic efficiency. Platooning is a concept within vehicle automation where a group of vehicles travels in a convoy on a highway, with a high level of automation and a small longitudinal distance in between. The aim is to achieve benefits in terms of fuel and traffic efficiency, safety and driver comfort. Studies have shown that the reduction of air drag, as a consequence of a short intermediate distance between HDVs in a platoon, decreases the fuel consumption by up to 12% [3][4][5][6][7].

A central challenge within platooning is the well-studied string stability issue. String stability issues can occur when vehicles in the platoon make decisions based purely on their direct preceding vehicle, and thus metaphorically forming a string. This can cause unstable behaviour where "errors on errors" of leader-initiated maneuvers accumulate throughout the platoon [8], which may cause vehicles further down in the platoon to leave the desired lane causing potentially very dangerous situations.

Moreover, in order for an HDV to operate autonomously, it needs to perceive its environment and itself, i.e. the road and its position in relation to it. Such sensor-based perception systems are prone to unforeseen failures, often caused by uncontrollable external factors such as pools of water on e.g. lane markings. Perception systems need to be robust against these kinds of sensor failures. In the case of a lateral control system, the camera sensor detecting lane markings, V2V-communication and distance-reading radar sensor are of particular interest.

## 1.2 Problem formulation and objectives

The purpose of this master's thesis is to develop a lateral control system that autonomously controls the lateral movement of heavy duty vehicles in a platoon. Autonomous control of the lateral movement has the potential of being superior to that of a human driver, enabling smaller inter-vehicular distances in a platoon. The objectives are to

- identify which sensor information and V2V communication is needed to generate reference signals to a lateral control system
- decide what control strategy is suitable for this application
- design, implement and evaluate the control system in a simulation environment
- be able to handle specific sensor failures.

The lateral control system is tested on high-fidelity vehicle models in a simulation environment called PreScan, which is more described in section 4.5.2. In addition, to generate a more robust control system, the quality of the sensor readings needs to be considered. As an example, Figure 1.1 shows recorded log data from the camera sensor measuring the distance to the lane markings which shows clear spikes in the data and the need of a filter.

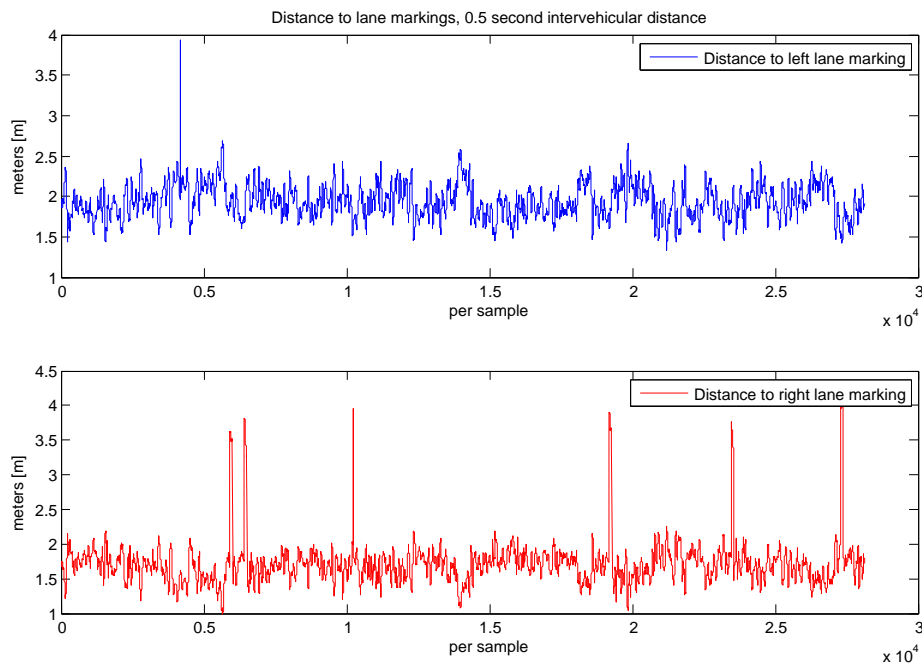


**Figure 1.1:** Log data, recorded at Hällered, from the camera lane marker sensor showing distance to left (top) and right (bottom) lane markings. Spikes, sensor failures, can be seen on both sides, especially right. These exemplify the need for somehow treating the sensor data before giving it to the control system.

To clarify further, a spike is zoomed in and displayed in Figure 1.2. These kind of failures can be caught by the confidence value of each measurement given by the camera and are of focus in this thesis. There are other types of sensor failures which are not as easily detectable and are not in the scope of this thesis.

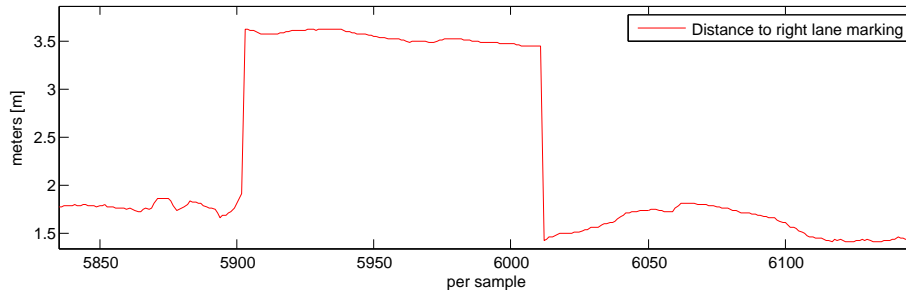


**Figure 1.2:** Zoom of the right lane marking distance above, illuminating a sensor failure. The failure could be that the camera picks up another object to track, or blockage of the correct lane marking.

### 1.3 Scope and limitations

The scope of this thesis lies on the development of the lateral control system for a platoon. Longitudinal dynamics, such as accelerating, breaking or non-zero road gradients, are outside the scope of this thesis. Thus, a constant longitudinal velocity and a constant inter-vehicular distance between each vehicle is assumed. Furthermore, the platoon scenario in focus is on highway driving. Modern highways have curve radii greater than 500 meter [9]. Vehicles that are not members of the platoon are considered absent and not taken into consideration. Driving situations that require leaving the lane are not considered.

### 1.4 Choice of control strategy

There are different approaches used in the literature to develop control systems for platooning. The most significant difference between the different approaches is whether or not they are using vehicle-to-vehicle (V2V) communication to send information. A platoon without V2V communication is often referred to as a local approach and a platoon which uses V2V is referred to as a global approach [10]. Although a local approach is robust in the sense that it does not rely on stable V2V communication, it does not give the same benefits as a global approach. The benefits of a global approach is the possibility to share information, which can e.g. give a larger look-ahead distance, since a small inter-vehicle distance may block the lane detection of the following vehicles, i.e. the back of the preceding vehicle takes up most of the following vehicles field of vision. Furthermore, another possibility with the global approach is to let all vehicles in the platoon share the same reference trajectory from the leading vehicle, thus making it possible to remove the string stability issues [11].

Furthermore, different control strategies are used in the literature, mainly PID control [12], Linear Quadratic (LQ) control [13] and Model Predictive Control (MPC) [14][9]. In order to utilize the knowledge of how the road looks ahead (obtained through V2V), a PID approach was put aside in favor of a more predictive approach, such as a LQR or an MPC controller. Taking into account that the road is a constrained environment and that an HDV has constrained steering, together with the importance of safety in a platoon, MPC, which has the strength of constraints, was deemed favorable over LQR.

Constraints used in model predictive controllers typically model control saturations. In the vehicle-case however, actual saturation of the steer wheel is not usual. However, constraints can be used to limit steering wheel angle to its typical operating region, and the rate of change of it, in order to prevent violent control actions that can be dangerous or uncomfortable. Constraints can further be used, in combination with lane detection, to keep the HDVs within a specific region, e.g. between the lane markings. More details about MPC and constraints can be found in Chapter 2.

### 1.4.1 MPC methods in platooning

Two main ways of implementing an MPC based control system for a platoon are found in the literature, namely centralized MPC and decentralized MPC. An MPC is considered to be implemented in a centralized manner when one MPC calculates the control signals for *all* vehicles in the platoon. Conversely, a decentralized implementation is when each vehicle only calculates its own control signal. The trade-off is between optimality, where centralized is superior, versus fast computation, where decentralized is superior. Since a centralized MPC is a more computationally demanding control strategy [14], a *global decentralized* MPC is used in this thesis.

## 1.5 Thesis outline

The outline is as follows. Chapter 2 reviews relevant theory used in the thesis. Chapter 3 describes how the platoon is set up in a more detailed manner, how the controllers references are built up, how the vehicles' and their positions relative to the road are modelled and what sensors are used. Chapter 4 shows how the MPC and Kalman filters are implemented and how sensor failures are modelled. It also describes the simulation environment. Chapter 5 shows the results of the simulations. Chapter 6 discusses the results. Chapter 7 contains a conclusion of the thesis. Chapter 8 gives relevant notes on the most central future work.

# 2

## Theoretical background

This chapter outlines the used theory, where the model predictive control approach is explained, and how to manipulate the standard formulation in a way to make control more smooth, how to add slack variables, how to use feed forward in the prediction model and also the theory of the linear Kalman filtering.

### 2.1 Model Predictive Control

A model predictive controller is at its core an online algorithm that uses a model to predict the future system behaviour and returns control signals based on numerical optimization in the form of minimizing a constrained quadratic cost function.

#### Prediction

The prediction model is used to describe the future behaviour of the system. In this thesis a linear MPC is used, a discrete-time state-space representation of the prediction model is written as follows

$$z(k+1) = A_d z(k) + B_d u(k) \quad (2.1)$$

where  $u(k)$  are the control inputs and  $z(k)$  the states at sample time  $k$ . Further,  $A_d$  is the discrete system matrix and  $B_d$  the discrete input matrix. The behaviour of the system is predicted  $N$  steps into the future, called the *prediction horizon*, using a predicted input sequence called the *control horizon* as follows

$$z(k+1+i|k) = A_d z(k+i|k) + B_d u(k+i|k) \quad i = 0, 1, \dots, N-1 \quad (2.2)$$

where  $z(k+i|k)$  and  $u(k+i|k)$  denote the values of the states and inputs at time  $k+i$  predicted at time  $k$ . The control horizon is typically the same as the prediction horizon, but can be made shorter in order to reduce the computational complexity. If made shorter, the last control input is usually kept for the remainder of the prediction horizon, i.e.  $u(k+N_u+i) = u(k+N_u)$  where  $N_u$  being the control horizon.

#### Optimization

The prediction of the states and the control inputs are then minimized in a cost function  $J$  which in this thesis is a quadratic cost function

$$J(k) = \sum_{i=0}^{N_h-1} \|z(k+1+i) - z_{ref}(k+1+i)\|_Q^2 + \sum_{i=0}^{N_u-1} \|u(k+i) - u_{ref}(k+i)\|_R^2 \quad (2.3)$$

where  $Q$  and  $R$  are positive definite matrices that contain scalar weights on the states and control inputs,  $z_{ref}$  future references of the states to be followed and  $u_{ref}$  future input references often set to zero. Minimizing the quadratic cost function yields the optimal sequence of control inputs  $u^*(k)$  at time  $k$

$$u^*(k) = \min_u J(k). \quad (2.4)$$

The cost function is also subject to the system constraints (2.1) and possibly further constraints on the states and the control inputs yielding the optimization problem

$$\begin{aligned} \min_u J(k) = \min_u & \sum_{i=0}^{N_h-1} \|z(k+1+i) - z_{ref}(k+1+i)\|_Q^2 + \\ & \sum_{i=0}^{N_u-1} \|u(k+i) - u_{ref}(k+i)\|_R^2 \\ \text{subject to: } & x(0) = x_0 \\ \forall i \in [0, N_h] : & z(k+1+i) = Az(k+i) + Bu(k+i) \\ \forall i \in [0, N_h] : & z(k+i) \in \mathcal{Z} \\ \forall i \in [0, N_h] : & u(k+i) \in \mathcal{U} \end{aligned} \quad (2.5)$$

where  $\mathcal{Z}$  is the additional set of constraints imposed on the states and  $\mathcal{U}$  are the constraints imposed on the control signals.

### Receding horizon framework

In an online computation of the algorithm, the minimization in (2.5) is solved at each sampling instant  $k$  generating the vector of optimal control inputs  $u^*(k)$  and only the first control input in this vector is applied to the actual plant, i.e.  $u(k) = u^*(k|k)$ . This is repeated for each sampling instant  $k = 0, 1, \dots$ . The online procedure of an MPC algorithm can be seen in Algorithm 1. The length of prediction horizon remains the same throughout each minimization of the algorithm thus creating a **receding** or **moving horizon**.

---

#### Algorithm 1 The MPC algorithm

---

1. Measure  $x(k|k)$
  2. Calculate control signals  $u$  by solving (2.5)
  3. Apply first control signal to actual plant
  4. Wait until next time instant, i.e. until  $k:=k+1$
  5. Repeat from 1.
-

## 2.2 Smooth Control

Large changes from a control signal to its consecutive one,  $\Delta u(k) = u(k) - u(k-1)$ , are both unrealistic, uncomfortable and potentially dangerous and thus sought to be minimized. This section describes how to limit changes of  $u(k)$  and  $\Delta u(k)$ .

### 2.2.1 Limiting changes of $u(k)$

To get more natural and smooth control, the prediction model can be changed to use control increments as input, i.e.  $\Delta u(k)$ , instead of  $u(k)$ . By doing so, it is straight forward to limit this increment, and thereby limiting how much  $u(k)$  can change between samples. In other words to go from

$$z(k+1) = A_d z(k) + B_d u(k) \quad (2.6)$$

where  $u(k)$  is the control input, to

$$\begin{bmatrix} z(k+1) \\ u(k) \end{bmatrix} = \underbrace{\begin{bmatrix} A_d & B_d \\ 0 & 1 \end{bmatrix}}_{\hat{A}} \underbrace{\begin{bmatrix} z(k) \\ u(k-1) \end{bmatrix}}_{\hat{z}(k)} + \underbrace{\begin{bmatrix} B_d \\ 1 \end{bmatrix}}_{\hat{B}} \Delta u(k) \quad (2.7)$$

where  $\Delta u(k)$  is the control increment, or control move.

### 2.2.2 Limiting changes of $\Delta u(k)$

Improving smoothness even more can be achieved by limiting the change between two consecutive control increments  $\Delta u$ , i.e.  $\Delta \Delta u(k) = \Delta u(k) - \Delta u(k-1) := \Delta^2 u(k)$ . By rearranging the following two relations

$$\begin{cases} \Delta u(k) = u(k) - u(k-1) \iff u(k) = \Delta u(k) + u(k-1) \\ \Delta^2 u(k) = \Delta u(k) - \Delta u(k-1) \iff \Delta u(k) = \Delta^2 u(k) + \Delta u(k-1) \end{cases}$$

an expression for  $u(k)$  can be obtained. After rearranging, the expression for  $u(k)$  is as follows

$$u(k) = u(k-1) + \Delta u(k-1) + \Delta^2 u(k). \quad (2.8)$$

Now using  $\Delta^2 u(k)$  as control input, the linear system can be expressed with the augmented state vector  $\xi = [z(k+1) \ u(k) \ \Delta u(k)]^T$  with the discrete-time state-space matrices

$$\mathcal{A} = \begin{bmatrix} A_d & B_d & B_d \\ 0 & 1 & 1 \\ 0 & 0 & 1 \end{bmatrix}, \quad \mathcal{B} = \begin{bmatrix} B_d \\ 1 \\ 1 \end{bmatrix}. \quad (2.9)$$

When limiting changes of  $u(k)$  and  $\Delta u(k)$ , the state-space representation (2.1) can be updated to

$$\xi^+ = \mathcal{A}\xi + \mathcal{B}\Delta^2 u. \quad (2.10)$$

### 2.3 Constraint management

Hard constraints often cause problems due to the mismatch between the prediction model and the actual plant. The MPC-generated trajectory may get close to the constraint and remain there, but the actual plant may slightly overshoot the trajectory and go outside of the constrained area, from where no feasible optimization can be found. A way to handle this is to soften the constraints by increasing their magnitudes with non-negative slack variables  $\varepsilon_{1:N}$ . The slack variables  $\varepsilon_{1:N}$  are added in the cost function  $J$  with a weight matrix  $S \in \mathbb{R}^{i \times i}$  in order to minimize them if possible. The weight matrix  $S$  is chosen much greater than  $Q$  and  $R$  in order to keep the slack variables at 0, and thus use the constraints as they originally were stipulated, unless anything else than increasing  $\varepsilon_i$  would result in infeasibility. Mathematically, a constraint which keeps a state  $z_1(k)$  over the prediction horizon  $k = 1, \dots, N_h - 1$  between a constant minimum and maximum value can be written as

$$z_{1_{min}} \leq z_1(k) \leq z_{1_{max}} \quad (2.11)$$

and when introducing slack variables reformulated into

$$z_{1_{min}} - \epsilon(k) \leq z_1(k) \leq z_{1_{max}} + \epsilon(k), \quad k = 1, \dots, N_h - 1. \quad (2.12)$$

The updated cost function, now containing the slack variables in the minimization, is written as

$$\begin{aligned} J(k) = & \sum_{i=0}^{N_h-1} \|z(k+1+i) - z_{ref}(k+1+i)\|_Q^2 + \\ & \|\epsilon(k+1+i)\|_S^2 + \\ & \sum_{i=0}^{N_u-1} \|u(k+i) - u_{ref}(k+i)\|_R^2. \end{aligned} \quad (2.13)$$

### 2.4 Utilizing preview information

Disturbances that act on states can be expressed by extending (2.10) with a disturbance  $\kappa$  with disturbance matrix  $W$ , i.e.

$$\begin{aligned} \xi_{k+1} &= \mathcal{A}\xi_k + \mathcal{B}\Delta^2 u_k + W\kappa_k \\ \xi_{k+2} &= \mathcal{A}\xi_{k+1} + \mathcal{B}\Delta^2 u_{k+1} + W\kappa_{k+1} \\ &\vdots \\ \xi_{k+N_h} &= \mathcal{A}\xi_{k+N_h-1} + \mathcal{B}\Delta^2 u_{k+N_h-1} + W\kappa_{k+N_h-1}. \end{aligned} \quad (2.14)$$

If the coming disturbances  $\kappa_k \dots \kappa_{N_h}$  are known, they can be accounted for by the MPC. Utilizing preview information in this manner is usually called feed forward.

## 2.5 Kalman filter

Measurements from sensors always contain an uncertainty, i.e. noise. Looking at a noisy reading of e.g. a vehicles position, one can be certain that the data one is looking at is untrue, since the vehicle still abides by the laws of physics and cannot make the, sometimes, momentaneous large changes in position that noisy data can indicate.

The Kalman Filter is a filter which estimates the states of a dynamic linear system based on measurements [15]. The idea is to take into account a process model which is a set of mathematical equations describing the states to be estimated, and combine the evolution of this process model with measurements to get a more accurate reading. The process model is typically written as (2.1), with the addition of process noise  $\omega$  to incorporate the uncertainty in the mathematical equations

$$z_k = Az_{k-1} + Bu_k + \omega_k \quad (2.15)$$

where  $\omega$  is assumed to be zero-mean white noise with covariance matrix  $Q$ , i.e.  $W \sim \mathcal{N}(0, Q)$ . The measurement of the true state is modelled through

$$y_k = Cz_k + v_k \quad (2.16)$$

where  $C$  is the measurement matrix mapping the true states  $z_k$  to the measurement observations  $y_k$ . Further,  $v_k$  is the measurement noise which is a zero-mean white noise with covariance matrix  $R$ . An iteration of the recursive filter has two steps, namely a prediction update step and a measurement update step. The outputs in each iteration are the mean values of the estimated states  $\hat{z}_k$  along with their covariance matrix  $P_k$ . An online algorithm of the Kalman filter can be seen in Algorithm 2.

---

### Algorithm 2 The Kalman filter algorithm

---

```

Initial prediction of state estimation based on  $z_0$ :  $z_k = Az_0 + Bu_0$ 
Initial prediction of covariance estimation based on  $P_0$ :  $P_k = P_0AP_0 + Q_k$ 
while measuring do
  Calculation of measurement residual:  $\tilde{y} = y_k - C\hat{z}_k$ 
  Calculation of optimal Kalman gain:  $K_k = P_kC(CPC^T + R_k)^{-1}$ 
  Correction of state estimation based on measurements:  $\hat{x}_k = \hat{z}_k + K_k\tilde{y}_k$ 
  Correction of covariance estimation based on measurements:  $P_k = (I - K_kC)P_k$ 
  Prediction of state estimation:  $\hat{z}_k = Az_{k-1} + Bu_{k-1}$ 
  Prediction of covariance estimation:  $P_k = P_{k-1}AP_{k-1} + Q_k$ 
return  $\hat{z}_k$ 
return  $P_k$ 
  k  $\leftarrow$  k+1
end while

```

---

## 2. Theoretical background

---

# 3

## System Description

This chapter explains the platoon setup in a more technical manner, the generation of the reference trajectories, the modelling of the lateral vehicle dynamics, the modelling of the lateral position dynamics w.r.t. the road and the discretization of the full dynamic model.

### 3.1 Platoon setup

The platoon under consideration consists of a leading vehicle which is steered manually by a driver and a number of following vehicles which are driven autonomously, see Figure 3.1.

The objective of the platoon is to follow behind each other in close distance, to receive the benefits in terms of air drag reduction, while being able to avoid obstacles within its lane. The vehicles are equipped with a camera measuring the lane markings, a radar measuring the distance to the preceding vehicle and antennas to be able to use V2V communication through a CAN bus coupled with a WiFi connection, described more in Section 3.4. It is assumed that each vehicle has a constant local longitudinal velocity  $\dot{x}$  of 20 m/s with a constant time headway front-to-bumper between each vehicle of 0.5 seconds as well as 1.0 seconds front-to-front. This assumption is based on log data provided from Volvo, where the minimal time headway was 0.5 seconds. Keeping the velocity  $\dot{x}$  and time headway between each vehicle constant is achieved by the related functionality Cooperative Adaptive Cruise Control (CACC) on flat roads. The platoon is assumed to operate on modern highways, which have curve radii greater than 500 meters. Furthermore, each following vehicle has a decentralized MPC calculating its own control signal based on its current position in the lane as well as the reference trajectory and curvature received from V2V. The sample time  $T_s$  for a HDV needs to be 50 ms or smaller to function as intended [16], and thus  $T_s$  is chosen to be 50 ms. The length of the prediction horizon needs to match the lengths front-to-front, thereby the number of prediction steps are chosen to be  $Headway/T_s = 20$  steps.

Two different global approaches are investigated, one where each vehicle follows its first preceding vehicle and one where each vehicle follow the manually steered leading vehicle. These approaches are described in more details in Section 3.2. In both approaches, the reference trajectories consists of the distance to the lane centerline  $y_{cl}$  and the heading between the vehicle and the lane centerline  $\Psi_{cl}$ . The curvature  $\kappa$  is sent at the same time as a feed forward addition and will tell each MPC in the following vehicles that a curvature is coming ahead of time, yielding a

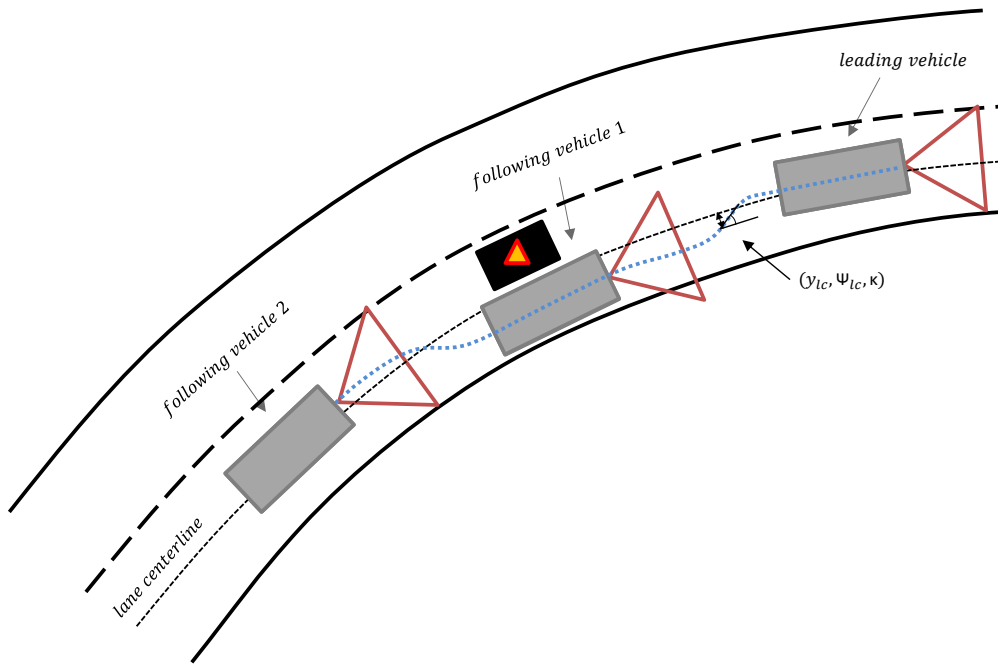


**Figure 3.1:** Overview of a platoon with one leading vehicle and two following vehicles. The objective of the platoon is to follow behind each other as well as avoiding objects within its lane. The red triangles visualize an approximation of the field of view of the camera sensors. The blue dots represent way points where the leading vehicle has travelled. Each of these blue dots contain information about the curvature  $\kappa$ , lateral offset  $y_{cl}$  and heading angle  $\Psi_{cl}$  indicated by the black arrow. The black box with a warning triangle visualizes an obstacle which needs to be avoided.

smoother transition from a straight road to a curved road. The curvature is treated as an input disturbance in the prediction model, which means that in each time step of the prediction horizon, the curvature of the road is taken into account as seen in (2.14). The continuous-time state-space representation of the prediction model is written as

$$\dot{z} = Az + Bu + W\kappa \quad (3.1)$$

where  $z$  are the states,  $u$  the control input and  $\kappa$  the input disturbance. The modelling of the prediction model is described in more details in Section 3.3.

## 3.2 Reference generation

This section describes the two different global approaches that are used to generate the references to the controllers in the platoon. In the first approach each vehicle follows its preceding vehicle, whereas in the second approach each vehicle follows the leading vehicle.

### 3.2.1 Reference generation based on preceding vehicle

In this approach, each vehicle transmits its position  $y_{cl}$  and heading relative to the lane  $\Psi_{cl}$  as well as the feed forward disturbance  $\kappa$  to their first succeeding vehicle. Figure 3.2 shows a platoon with three vehicles with the first being the leading vehicle.

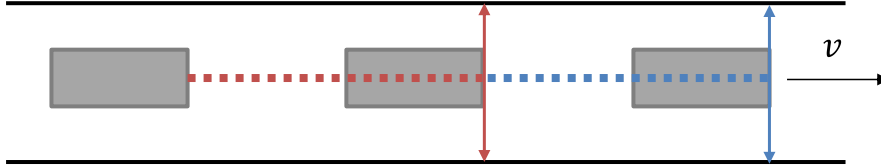


**Figure 3.2:** A three-vehicle platoon with two following vehicles and one leading vehicle using preceding vehicle approach. The dotted blue and red lines indicates the reference trajectories of the first respectively second follower in the platoon.

The reference trajectory for the first following vehicle is represented by the blue dots, and the reference trajectory for the second following vehicle is represented by the red dots. These trajectories have fixed length, starting at its own camera ending at their preceding vehicle's camera. Thus, each dot in the trajectory stores a future reference at that current position on the road with a distance to the lane centerline  $y_{cl}$  and heading  $\Psi_{cl}$ . The time-length of the reference trajectory is equal to  $N \cdot T_s$  where  $N$  is the number of waypoints and  $T_s$  the sampling time of the MPCs, as described in Section 3.1. These reference trajectories are updated every sampling instant  $T_s$  giving each MPC a possibly completely new reference trajectory. The reference trajectories of three following vehicles are visualized in Figure 3.3.

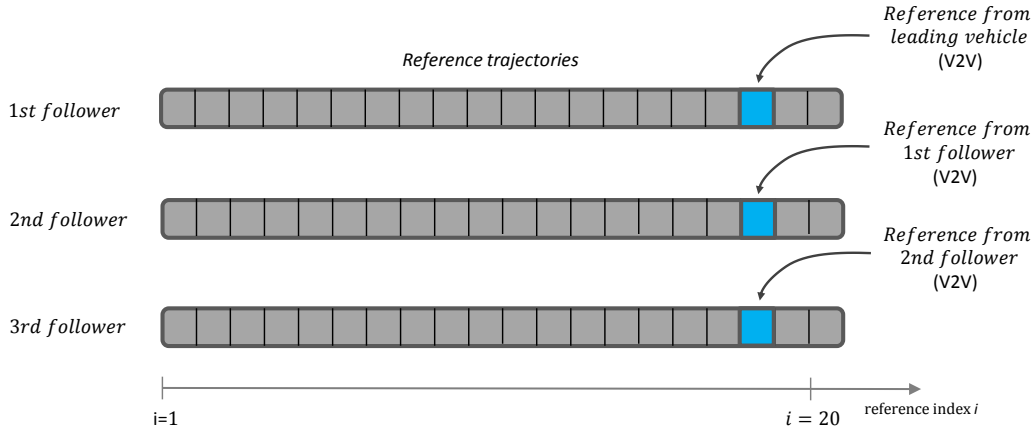


**Figure 3.3:** Visual representation of how the reference trajectory in each MPC is updated using preceding vehicle approach, when accounting for a known, constant V2V delay. In each time step, the trajectories are shifted one time step to the left removing the oldest and just passed reference entries ( $i = 1$ ) after which newly acquired references at the end of each trajectory ( $i = 18$ ) is added. Reference trajectories is of length 20, sample time of 0.05 s and V2V delay of 0.1 s.

In each sampling instant, each reference trajectory is shifted one step to the left removing the waypoints just passed by each vehicle which corresponds to index  $i = 1$  after which new waypoints are added in the end of each trajectory. To account for V2V delay, which is approximated as a constant delay of 0.1 seconds and  $T_s$  being 0.05 seconds, the new waypoints are added two samples ahead. The new waypoints are indicated by blue color and are added at position index  $i = 18$ .

#### 3.2.2 Reference generation based on leading vehicle

In this approach, each vehicle will instead follow the leading vehicle, where the leading vehicle transmits the same references  $y_{cl}$  and  $\Psi_{cl}$  together with the feed forward disturbance  $\kappa$  as the previous approach. Figure 3.4 show the same platoon scenario with three vehicles with the difference being that the data in the reference trajectories will all originate from the leading vehicle, indicated by blue color.

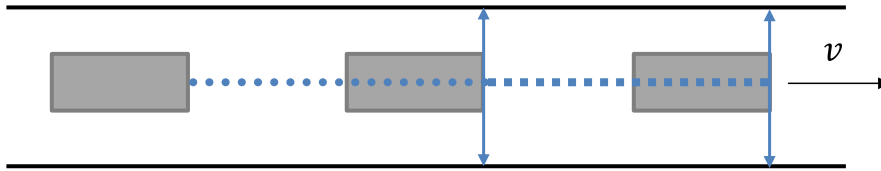


**Figure 3.4:** A three-vehicle platoon with two following vehicles and one leading vehicle using leading vehicle approach. The squared and circled blue lines indicates the reference trajectories of the first respectively second follower in the platoon.

Each vehicle will still transmit a waypoint at each sample time  $T_s$  to its first succeeding vehicle as before, but the waypoint will no longer be based on its own camera. Instead, the waypoints originate from the leading vehicle and are passed through each vehicle. The reference trajectories have the same length  $N = 20$  visualized with blue squares and blue circles for the first and second follower respectively. The reference trajectories are starting from the corresponding vehicles camera reaching to the preceding vehicles camera. How the reference trajectories are generated can be seen in Figure 3.5. At each sampling instant  $T_s$  the first follower will pass through a waypoint at reference index  $i = 3$  in its reference trajectory to the second follower where a constant delay of 0.1 seconds is taken into account. The whole trajectory is afterwards in the same sampling time  $T_s$  shifted one time step to the left removing the oldest reference entry  $i = 1$ . The leading vehicle will then send a new waypoint to the first following vehicle to reference index  $i = 18$  indicated by blue color where a constant delay of 0.1 seconds is yet again considered. This pattern then repeats itself along the platoon members.

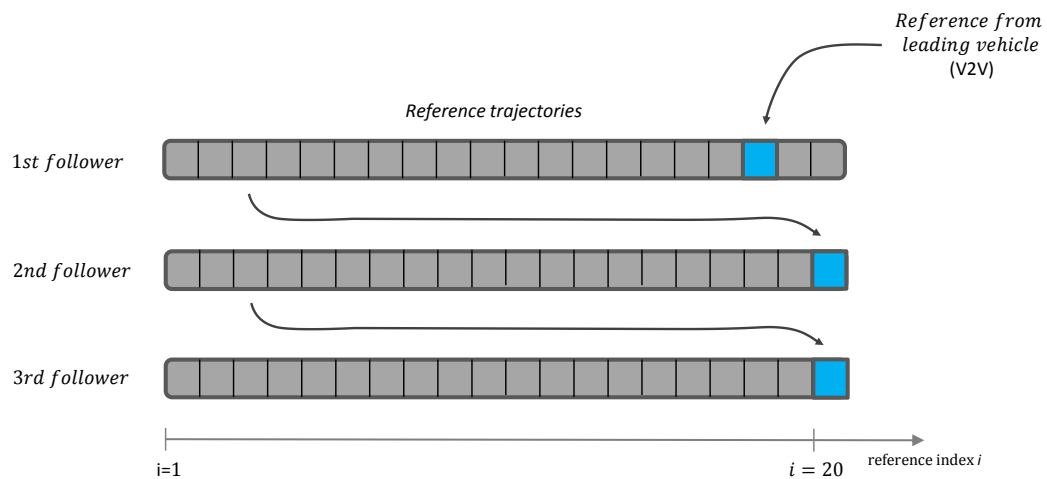


**Figure 3.5:** Visual representation of how the reference trajectory in each MPC is updated using the leading vehicle approach, when accounting for a known, constant V2V delay. In each time step, the vectors are shifted one time step to the left removing the oldest and just passed reference entries ( $i = 1$ ) after which a new acquired reference is added to the first follower ( $i = 18$ ) which then also forwards a new reference to its succeeding follower (to  $i = 20$ ) in the same manner. Reference trajectories of length 20, sample time of 0.05 seconds and V2V delay of 0.1 seconds.

### 3.3 Modelling

This section describes the modelling of the lateral vehicle dynamics, based on [17], as well as the modelling of the lateral position dynamics relative to the road.

#### 3.3.1 Lateral vehicle dynamics

What one gets if the distance between the pair of tires on each axle is reduced to zero is intuitively called a bicycle model. The bicycle model is often sufficient and recommended to use if the radii of the roads are large, since it only considers lateral and yaw motion, and no roll motion. The states of the bicycle model used in this thesis are the local lateral velocity  $\dot{y}$  and the angular velocity  $\dot{\Psi}$ . The modelled bicycle can be seen in Figure 3.6.

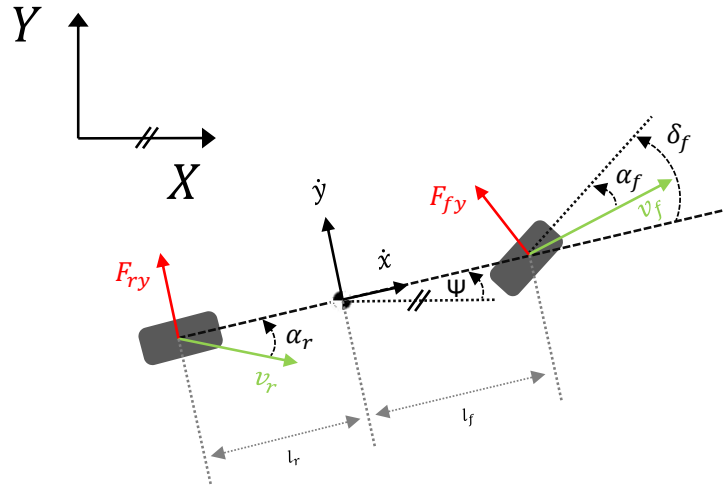


**Figure 3.6:** Bicycle model showing lateral forces  $F_{ry}$  and  $F_{fy}$ , slip angles  $\alpha_r$  and  $\alpha_f$ , steering wheel angle  $\delta_f$ , tire rear and front velocity vectors  $v_r$  and  $v_f$ , local longitudinal and lateral velocities  $\dot{x}$  and  $\dot{y}$  and finally yaw angle  $\Psi$  w.r.t. the global coordinate frame. The distances to the center of gravity from the rear and front axle are called  $l_r$  and  $l_f$  respectively.

The total lateral force on the two-wheeled bicycle model is, neglecting air drag, the sum of the lateral forces from the front and rear tire as seen in Figure 3.6, assuming small steering angle  $\delta_f$ . The total lateral acceleration is the acceleration along the vehicles  $y$ -axis and the centripetal force. Using Newtons second law the following equations are derived

$$ma_y = F_{ry} + F_{fy} \quad (3.2)$$

$$a_y = \ddot{y} + \dot{x}\dot{\Psi} \quad (3.3)$$

where  $m$  is the total mass,  $a_y$  the total lateral acceleration,  $F_{ry}$  and  $F_{fy}$  the rear and front lateral forces respectively, and  $\dot{x}$  the local longitudinal velocity.

Combining (3.2) and (3.3) yields

$$m(\ddot{y} + \dot{x}\dot{\Psi}) = F_{ry} + F_{fy}. \quad (3.4)$$

The lateral tire forces  $F_{fy}$  and  $F_{ry}$  have, experimentally, been shown to be proportional to the angle between the tire orientations and the velocity vectors  $v_{\{f,r\}}$  of the vehicle if that angle is small as follows

$$F_{ry} = 2C_r\alpha_r \quad (3.5)$$

$$F_{fy} = 2C_f\alpha_f \quad (3.6)$$

where  $\alpha_{\{r,f\}}$  are called the tire slip angles and  $C_{\{r,f\}}$  the cornering stiffnesses given per tire for the rear and front axle respectively. The tire slip angles  $\alpha_{\{r,f\}}$  can in turn be written as

$$\alpha_r = -\beta_r \quad (3.7)$$

$$\alpha_f = \delta_f - \beta_f \quad (3.8)$$

where  $\beta_{\{r,f\}}$  are the side slip angles for front and rear tire respectively. The angles  $\beta_{\{r,f\}}$  are the tangent of the lateral velocity vector components  $v_{\{r,f\}}$  divided by the longitudinal velocity vector component  $\dot{x}$ . Using a small angle approximation gives the following relationships for  $\beta_{\{r,f\}}$

$$\tan(\beta_r) \approx \beta_r = \frac{\dot{y} - l_r\dot{\Psi}}{\dot{x}} \quad (3.9)$$

$$\tan(\beta_f) \approx \beta_f = \frac{\dot{y} + l_f\dot{\Psi}}{\dot{x}} \quad (3.10)$$

where  $l_r$  and  $l_f$  are the distances to the center of gravity from the rear and front axle respectively. Now, inserting (3.10) and (3.9) in (3.8) and (3.7) respectively, and the obtained equations in (3.5) and (3.6), the lateral forces can be written as

$$F_{ry} = 2C_r\left(\frac{-\dot{y} + l_r\dot{\Psi}}{\dot{x}}\right) \quad (3.11)$$

$$F_{fy} = 2C_f\left(\delta - \frac{\dot{y} + l_f\dot{\Psi}}{\dot{x}}\right). \quad (3.12)$$

Using (3.11) and (3.12) in (3.4) yields a final expression for the lateral acceleration

$$\ddot{y} = \frac{C_f + C_r}{m\dot{x}}\dot{y} - \frac{C_f l_f - C_r l_r}{m\dot{x}}\dot{\Psi} - \dot{x}\dot{\Psi} + \frac{C_f}{m}\delta_f. \quad (3.13)$$

For the angular acceleration  $\ddot{\Psi}$ , a moment balance about the vehicles z-axis is first considered

$$I_z\ddot{\Psi} = l_f F_{fy} - l_r F_{ry} \quad (3.14)$$

where  $I_z$  is the moment inertia around z-axis. Using (3.11) and (3.12) again in (3.14) gives a final expression for the angular acceleration

$$\ddot{\Psi} = -\frac{(C_f l_f - C_r l_r)}{I_z \dot{x}} \dot{y} - \frac{C_f l_f^2 + C_r l_r^2}{I_z \dot{x}} \dot{\Psi} + \frac{C_f l_f}{I_z} \delta_f. \quad (3.15)$$

Finally, using the state equations (3.13) and (3.15) in standard state space form yields

$$\begin{bmatrix} \ddot{y} \\ \ddot{\Psi} \end{bmatrix} = \begin{bmatrix} \frac{C_f + C_r}{m \dot{x}} & -\frac{C_f l_f - C_r l_r}{m \dot{x}} - \dot{x} \\ -\frac{(C_f l_f - C_r l_r)}{I_z \dot{x}} & -\frac{C_f l_f^2 + C_r l_r^2}{I_z \dot{x}} \end{bmatrix} \begin{bmatrix} \dot{y} \\ \dot{\Psi} \end{bmatrix} + \begin{bmatrix} \frac{C_f}{m} \\ \frac{C_f l_f}{I_z} \end{bmatrix} \delta_f. \quad (3.16)$$

### 3.3.2 Lateral position dynamics

In order to follow a reference from the leading vehicle and to keep each vehicle on the lane, the bicycle model needs to be extended. Figure 3.7 shows the modelling of the lateral position dynamics relative to the lane centerline. Similar approaches have been used with MPC in lane keeping systems [18][19] and in platooning [20]. The two states  $\Psi_{lc}$  and  $y_{lc}$  marked in red are added to the model. These states represent the heading angle between the vehicle and the road and the distance from the road centerline to the camera sensor, which is placed on the vehicles x-axis at the top of the cabin.

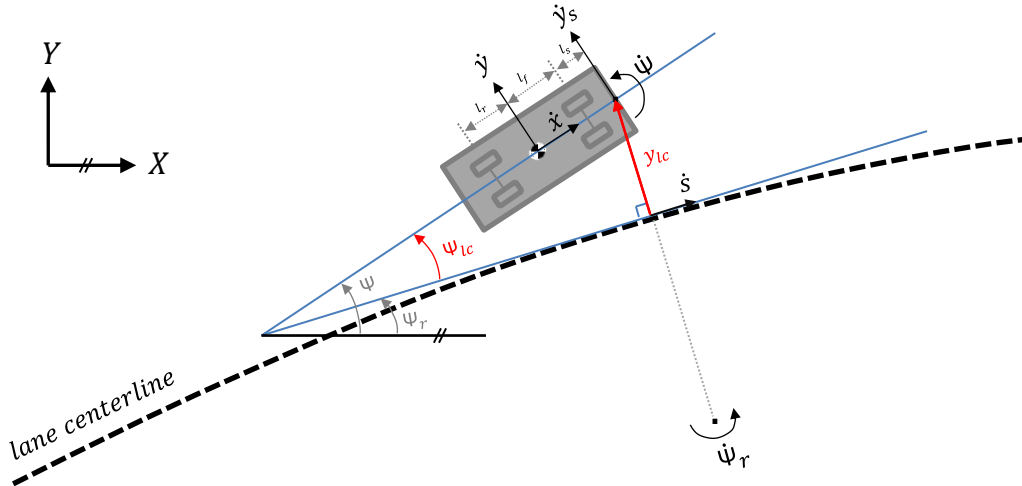


**Figure 3.7:** Modelling of the lateral position dynamics relative to the lane centerline. The bicycle model derived in 3.3.1 is extended with the states marked in red which are the distance to the lane centerline  $y_{lc}$  and the heading between the vehicle and the lane  $\Psi_{lc}$ .

The following nonlinear equations describes the lateral position dynamics

$$\dot{\Psi}_{lc} = \dot{\Psi} - \dot{\Psi}_r = \dot{\Psi} - \kappa \dot{s} \quad (3.17)$$

$$\dot{y}_{lc} = \dot{y}_s \cos(\Psi_{lc}) + \dot{x} \Psi_{lc} \quad (3.18)$$

$$\dot{s} = \dot{x} \cos(\Psi_{lc}) + \dot{y}_s \sin(\Psi_{lc}) \quad (3.19)$$

where  $\Psi$  and  $\Psi_r$  are the angles of the vehicle and the road respectively, relative to the global inertial frame. The yaw rate of the road  $\dot{\Psi}_r$  can be written as  $\kappa\dot{s}$  where  $\kappa$  is the curvature of the road. The velocity  $\dot{s}$  is the velocity tangent to the curve. Furthermore,  $\Psi_{lc}$  and  $y_{cl}$  are relative to the road aligned coordinate frame. The velocities  $\dot{x}$ ,  $\dot{y}$  and  $\dot{y}_s$  are the velocities of the vehicle in the body fixed coordinate frame. The velocity  $\dot{y}_s$  is rewritten as

$$\dot{y}_s = \dot{y} + (l_f + l_s)\dot{\Psi} \quad (3.20)$$

where  $l_s$  is the distance from the front axle to the camera sensor. Since the platoon is assumed to drive in a modern highway with  $radii > 500$  meters the angle  $\Psi_{lc}$  is small. With this approximation the nonlinear equations can be simplified to linear equations as follows

$$\begin{aligned} \dot{\Psi}_{lc} &= \dot{\Psi} - \dot{\Psi}_r = \dot{\Psi} - \kappa\dot{s} \\ \dot{y}_{lc} &= \dot{y} + (l_f + l_s)\dot{\Psi} + \dot{x}\Psi_{lc} \\ \dot{s} &= \dot{x}. \end{aligned} \quad (3.21)$$

This yields the final two linear equations for the lateral position dynamics

$$\begin{aligned} \dot{\Psi}_{lc} &= \dot{\Psi} - \kappa\dot{x} \\ \dot{y}_{lc} &= \dot{y} + (l_f + l_s)\dot{\Psi} + \dot{x}\Psi_{lc}. \end{aligned} \quad (3.22)$$

Writing the equations in (3.22) into state space form and using them together with the linear bicycle equations in (3.16) yields the following extended continuous state space model

$$\begin{bmatrix} \ddot{y} \\ \ddot{\Psi} \\ \dot{\Psi}_{cl} \\ \dot{y}_{cl} \end{bmatrix} = \begin{bmatrix} \frac{C_f + C_r}{m\dot{x}} & -\frac{C_f l_f - C_r l_r}{m\dot{x}} - \dot{x} & 0 & 0 \\ -\frac{(C_f l_f - C_r l_r)}{I_z \dot{x}} & -\frac{C_f l_f^2 + C_r l_r^2}{I_z \dot{x}} & 0 & 0 \\ 0 & 1 & 0 & 0 \\ 1 & l_f + l_s & \dot{x} & 0 \end{bmatrix} \begin{bmatrix} \dot{y} \\ \dot{\Psi} \\ \Psi_{lc} \\ y_{lc} \end{bmatrix} + \begin{bmatrix} \frac{C_f}{m} \\ \frac{C_f l_f}{I_z} \\ 0 \\ 0 \end{bmatrix} \delta_f + \begin{bmatrix} 0 \\ 0 \\ \dot{x} \\ 0 \end{bmatrix} \kappa \quad (3.23)$$

where the curvature  $\kappa$  is the feed forward input disturbance,  $A_c$  is the continuous system matrix and  $B_c$  the continuous input matrix. The discrete version of this continuous model can be regarded as the prediction model according to (2.1) in Section 2.1, although with the addition of curvature as an input disturbance described in Section 2.4. However, the full discrete model is described in Section 3.3.4.

### 3.3.3 Discretization

To find the analytical solution of a linear continuous system

$$\dot{x}(t) = A_c x(t) + B_c u(t) \quad (3.24)$$

the expression is first rearranged and then by introducing an integrating factor the following equation is found

$$e^{-A_c t} \dot{x}(t) - e^{-A_c t} A_c x(t) = e^{-A_c t} B_c u(t). \quad (3.25)$$

Further, the LHS is identified to have another form and is rewritten to

$$\frac{d}{dt}(e^{-A_c t} x(t)) = e^{-A_c t} B_c u(t). \quad (3.26)$$

Integrating both sides and rearranging with the follows steps

$$\int_{t_0}^t \frac{d}{dt}(e^{-A_c t} x(t)) d\tau = \int_{t_0}^t e^{-A_c \tau} B_c u(\tau) d\tau \quad (3.27)$$

$$e^{-A_c t} x(t) - e^{-A_c t_0} x(t_0) = \int_{t_0}^t e^{-A_c \tau} B_c u(\tau) d\tau \quad (3.28)$$

$$e^{-A_c t} x(t) = e^{-A_c t_0} x(t_0) + \int_{t_0}^t e^{-A_c \tau} B_c u(\tau) d\tau \quad (3.29)$$

$$x(t) = e^{A_c(t-t_0)} x(t_0) + \frac{1}{e^{-A_c t}} \int_{t_0}^t e^{-A_c \tau} B_c u(\tau) d\tau \quad (3.30)$$

yields the analytical solution

$$x(t) = e^{A_c(t-t_0)} x(t_0) + \int_{t_0}^t e^{A_c(t-\tau)} B_c u(\tau) d\tau. \quad (3.31)$$

Now using (3.31), the discrete solution is obtained by defining

$$x(t) := x(kT), \quad k = 0, 1, 2, \dots \quad (3.32)$$

with  $T$  as sampling period. The control signal  $u$  is assumed to be made continuous by being kept constant over a sampling period, i.e. zero order hold (ZOH). Inserting (3.32) in (3.31) with  $t_0 = kT$  and  $t = (k+1)T$  yields

$$x((k+1)T) = e^{A_c((k+1)T-kT)} x(kT) + \int_{kT}^{(k+1)T} e^{A_c((k+1)T-\tau)} B_c u(\tau) d\tau \quad (3.33)$$

where  $u$  is kept constant during one change of  $k$  since ZOH is in effect. This gives

$$x_{k+1} = e^{A_c T} x_k + \int_{kT}^{(k+1)T} e^{A_c((k+1)T-\tau)} B_c d\tau \cdot u_k \quad (3.34)$$

and changing variables to  $\Upsilon = (k+1)T - \tau$  gives

$$x_{k+1} = e^{A_c T} x_k + \int_0^T e^{A_c \Upsilon} B_c d\Upsilon \cdot u_k. \quad (3.35)$$

Comparing (3.35) with (3.24), the discrete time state-spaces matrices can be identified as

$$A_d = e^{A_c T} \quad (3.36)$$

$$B_d = \int_0^T e^{A_c \Upsilon} B_c d\Upsilon \quad (3.37)$$

$$(3.38)$$

which can be expressed as infinite sums. For implementation, this is closely approximated by finite sums (limiting the summation variable  $i$ ) which gives

$$A_d = e^{A_c T} \approx \sum_{i=0}^{i_{sufficient}} \frac{(A_c T)^i}{i!} \quad (3.39)$$

$$B_d = \int_0^T e^{A_c \Upsilon} B_c d\Upsilon \approx \sum_{i=0}^{i_{sufficient}} \frac{(A_c T)^i}{(i+1)!} B_c T. \quad (3.40)$$

$i_{sufficient}$  was found to be around 5 for this thesis case.

### 3.3.4 Discrete model

The full discrete model is obtained by discretizing the continuous model (3.23) with equations (3.39) and (3.40) and extending it with steering wheel acceleration as control input as described in Section 2.2. This gives the following full discrete model

$$\begin{bmatrix} z(k+1) \\ u(k) \\ \Delta u(k) \end{bmatrix} = \begin{bmatrix} A_d & B_d & B_d \\ 0 & 1 & 1 \\ 0 & 0 & 1 \end{bmatrix} \begin{bmatrix} z(k) \\ u(k-1) \\ \Delta u(k-1) \end{bmatrix} + \begin{bmatrix} B_d \\ 1 \\ 1 \end{bmatrix} \Delta^2 u(k) + \begin{bmatrix} W_d \\ 0 \\ 0 \end{bmatrix} \kappa(k) \quad (3.41)$$

which corresponds to (2.14) in Section 2.4.

## 3.4 Sensors

This section describes the sensors required for this platooning setup. The sensors used are cameras, radars, internal vehicle sensors, and V2V communication. The decision to use this combination of sensors was based on discussions with Volvo GTT.

### 3.4.1 Camera

There are four momentaneous quantities needed from the lane markings, taken perpendicular to the position of the forward-facing camera on each HDV. These quantities are the heading relative to the centerline of the lane  $\Psi_{cl}$ , the distance to the right and left lane markings (which combined can be used to find the distance to the centerline of the lane  $y_{cl}$ ) and the curvature  $\kappa$ .

### 3.4.2 Radar

The radar was noted to be better at measuring inter-vehicular distance than the camera. In the case of varying inter-vehicular distance, this can be used to stretch or shrink the time between each sample, i.e. the sampling time  $T_s$  in order to maintain the number of samples in the horizon.

### 3.4.3 Internal vehicle states

The predictive model derived above needs measurements of the local lateral velocity  $\dot{y}$ , the yaw rate  $\dot{\Psi}$  and local longitudinal velocity  $\dot{x}$ . The yaw rate is measured using a gyroscope and the longitudinal velocity is measured using a tachometer. The lateral velocity is estimated from the yaw rate measurements.

### 3.4.4 V2V

The V2V system that is used is realized through a CAN bus and a WiFi network. The V2V system can send arbitrary information between vehicles where all vehicles in the platoon are capable of sending and receiving. A delay of 100 *ms* is assumed between each transmission and its respective reception. Packet losses are not considered.

# 4

## Implementation

This chapter describes how the used MPCs and Kalman filters are tailored to the application and how the simulation setup is implemented. Additionally, modelling of lane marking losses is presented.

### 4.1 MPC formulation

The control objective of the optimization problem is to minimize the control signals such that the deviation from the reference trajectory  $y_{lc_{ref}}, \Psi_{lc_{ref}}$  transmitted from the leading vehicle is also minimized, while satisfying constraints on the states and inputs. The optimization problem has been formulated as

$$\underset{\Delta^2 u(0:N-1), \epsilon(1:N)}{\text{minimize}} \sum_{i=0}^{N-1} \|\eta(k+1+i) - \eta_{ref}(k+1+i)\|_Q^2 + \|\Delta^2 u(k+i)\|_R^2 + \|\epsilon(k+1+i)\|_S^2 \quad (4a)$$

subject to

$$\xi(k+1) = \mathcal{A}\xi(k) + \mathcal{B}\Delta^2 u(k) + W\kappa(k), \quad (4b)$$

$$\eta(k+1+i) = C\xi(k+1+i), \quad (4c)$$

$$u_{min} \leq u(k) \leq u_{max}, \quad (4d)$$

$$\Delta u_{min} \leq \Delta u(k) \leq \Delta u_{max}, \quad (4e)$$

$$\Delta^2 u_{min} \leq \Delta^2 u(k) \leq \Delta^2 u_{max}, \quad (4f)$$

$$y_{lc_{min}} - \epsilon(k+1) \leq y_{lc}(k+1) \leq y_{lc_{max}} + \epsilon(k+1), \quad (4g)$$

$$\epsilon(k+1) \geq 0, \quad (4h)$$

$$k = 0, \dots, N-1$$

where  $\eta = C\xi = [y_{lc} \ \Psi_{lc} \ u \ \Delta u]^T$  and where  $\Delta^2 u(0 : N-1) = [\Delta^2 u(0), \dots, \Delta^2 u(N-1)] \in \mathbb{R}^N$  is the set of future control signals and  $\epsilon(1 : N)$  are the slack variables. Furthermore,  $N$  is the prediction and control horizon,  $Q, R, S$  are positive definite weights on the states, control signals and slack variables. The optimization problem includes constraints on the state  $y_{lc}$  as in (4g) to avoid leaving the lane and also actuator limitations on the steering wheel angle, angular rate and angular acceleration as in (4d-4f) to avoid the risk of roll over. The optimization is solved at each time instant and the very first element of the set of future control signals  $\Delta^2 u(k)$  is used,

while the rest are discarded. The control signal  $\Delta^2 u(k)$  is then integrated twice and applied to the corresponding vehicle. This optimization is performed every sampling instant in each vehicle giving a new steering wheel angle 20 times per second.

### 4.1.1 FORCES Pro

FORCES Pro is a code generation tool [21] used for different optimization algorithms, including optimal control, which has been used in this thesis. The FORCES Pro tool requires the optimal control problem to be formulated in a standard form

$$\begin{aligned} & \text{minimize} && \sum_{i=1}^N \frac{1}{2} \chi_i^T H \chi_i + f_i^T \chi_i \\ & \text{subject to} && D_1 \chi_1 = c_1 \\ & && C_{i-1} \chi_{i-1} + D_i \chi_i = c_i \\ & && A \chi_i \leq b \end{aligned} \tag{4.1}$$

where  $\chi_i$  are the optimization variables,  $H$  the Hessian matrix containing weighting matrices and  $f_i$  the remaining linear terms.

## 4.2 MPC formulation in standard form

In order to use FORCES Pro, the optimization problem in (4a-h) needs to be formulated in standard form shown in (4.1). The optimization vector  $\chi$  will then be

$$\chi_i = [\Delta^2 u(k-1+i) \quad \xi(k+i) \quad \epsilon(k+i)]^T, \quad i = 1, \dots, N-1. \tag{4.2}$$

Furthermore, the Hessian matrix  $H$  will be a diagonal matrix as follows

$$H = \begin{bmatrix} R & 0 & 0 \\ 0 & Q & 0 \\ 0 & 0 & S \end{bmatrix} \tag{4.3}$$

containing the positive definite matrix  $Q$  and positive definite scalars  $R, S$  where  $Q$  is a  $6 \times 6$  matrix containing the weights of the states and  $R$  and  $S$  are two scalars weights for the control input  $\Delta^2 u$  and slack variable  $\epsilon$ . The remaining linear terms are collected in the vector  $f$

$$f_i = [-\Delta^2 u_{ref} R \quad -\xi_{i_{ref}}^T Q \quad -\epsilon_{ref} S]^T, \quad i = 1, \dots, N-1 \tag{4.4}$$

where  $\Delta^2 u_{ref} = 0$ ,  $\epsilon_{ref} = 0$  and

$$\xi_{i_{ref}}^T = [0 \quad 0 \quad \Psi_{l_{cref}}(k+i) \quad y_{l_{cref}}(k+i) \quad 0 \quad 0], \quad i = 1, \dots, N-1. \tag{4.5}$$

The equality constraints (4b-c) are transformed such that they fit the matrices  $C$  and  $D$ .

The matrix  $C$  is written as follows

$$C = \begin{bmatrix} \mathbf{0}_{4,1} & A_d & B_d & B_d \\ 0 & \mathbf{0}_{1,4} & 1 & 1 \\ 0 & \mathbf{0}_{1,4} & 0 & 1 \\ 0 & \mathbf{0}_{1,4} & 0 & 0 \end{bmatrix} \quad (4.6)$$

where  $A_d$  and  $B_d$  are the discretized prediction model matrices in (2.1) and  $\mathbf{0}_{i,j}$  a vector or matrix containing zeros with  $i$  rows and  $j$  columns. The matrix  $D$  is written as follows

$$D = \begin{bmatrix} B_d & -\mathbf{I}_4 & \mathbf{0}_{4,2} & \mathbf{0}_{4,1} \\ \mathbf{1}_{2,1} & \mathbf{0}_{2,4} & -\mathbf{I}_2 & \mathbf{0}_{2,1} \end{bmatrix} \quad (4.7)$$

where  $\mathbf{I}_i$  is the identity matrix of size  $i$ . Furthermore, the inequality constraints (4d-h) are written as

$$\underbrace{\begin{bmatrix} 0 & \mathbf{0}_{1,3} & 0 & -1 & 0 & 0 \\ 0 & \mathbf{0}_{1,3} & 0 & 1 & 0 & 0 \\ 0 & \mathbf{0}_{1,3} & 0 & 0 & -1 & 0 \\ 0 & \mathbf{0}_{1,3} & 0 & 0 & 1 & 0 \\ -1 & \mathbf{0}_{1,3} & 0 & 0 & 0 & 0 \\ 1 & \mathbf{0}_{1,3} & 0 & 0 & 0 & 0 \\ 0 & \mathbf{0}_{1,3} & -1 & 0 & 0 & 0 \\ 0 & \mathbf{0}_{1,3} & 1 & 0 & 0 & 0 \\ 0 & \mathbf{0}_{1,3} & 0 & 0 & 0 & -1 \end{bmatrix}}_A \chi_i \leq \underbrace{\begin{bmatrix} -u_{min} \\ u_{max} \\ -\Delta u_{min} \\ \Delta u_{max} \\ -\Delta^2 u_{min} \\ \Delta^2 u_{max} \\ -y_{lc_{min}} \\ y_{lc_{max}} \\ 0 \end{bmatrix}}_b. \quad (4.8)$$

Finally, the  $c$  matrix which contains the curvature and the initial condition is written as follows

$$\begin{cases} c_1 = - \begin{bmatrix} A_d & B_d & B_d \\ 0 & 1 & 1 \\ 0 & 0 & 1 \end{bmatrix} \xi(k) - \begin{bmatrix} W_d \\ 0 \\ 0 \end{bmatrix} \kappa_1 \\ c_i = - \begin{bmatrix} W_d \\ 0 \\ 0 \end{bmatrix} \kappa_i \end{cases} \quad (4.9)$$

where  $W_d$  is the disturbance matrix and  $\kappa_i$  the curvature for each step  $i = 2, \dots, N$  in the prediction horizon.

### 4.3 Kalman filters

This section describes how the Kalman Filters are implemented. The leading vehicle has a separate filter since it senses, in addition to what a following vehicle senses, the curvature  $\kappa$  of the road.

#### Leading vehicle Kalman filter

The same prediction model used in the MPCs are used in the leading vehicles Kalman filter, with the addition of the curvature  $\kappa$  as a state

$$\dot{\kappa} = 0 + v \quad (4.10)$$

where  $v$  is process noise. The process model of the leading vehicles Kalman filter is then the following

$$\begin{bmatrix} \ddot{y} \\ \ddot{\Psi} \\ \dot{\Psi}_{cl} \\ \dot{y}_{cl} \\ \dot{\kappa} \end{bmatrix} = \begin{bmatrix} \frac{C_f+C_r}{m\dot{x}} & -\frac{C_f l_f - C_r l_r}{m\dot{x}} - \dot{x} & 0 & 0 & 0 \\ -\frac{(C_f l_f - C_r l_r)}{I_z \dot{x}} & -\frac{C_f l_f^2 + C_r l_r^2}{I_z \dot{x}} & 0 & 0 & 0 \\ 0 & 1 & 0 & 0 & -\dot{x} \\ 1 & l_f + l_s & \dot{x} & 0 & 0 \\ 0 & 0 & 0 & 0 & 0 \end{bmatrix} \begin{bmatrix} \dot{y} \\ \dot{\Psi} \\ \Psi_{lc} \\ y_{lc} \\ \kappa \end{bmatrix} + \begin{bmatrix} \frac{C_f}{I_z} \\ \frac{C_f l_f}{I_z} \\ 0 \\ 0 \\ 0 \end{bmatrix} \delta \quad (4.11)$$

which is discretized with equations (3.39) and (3.40). Furthermore, all the states in (4.11) are measured and the measurement matrix  $C$  in (2.16) is the identity matrix  $I_5$ . The process noise and measurement noise in (2.15) and (2.16) respectively are zero-mean white noise with covariance matrix  $Q$  and  $R$ . The covariance matrices are both diagonal matrices where  $Q$  has been tuned experimentally and  $R$  contains variances of the state measurements from real data logs on a test track. The initial guess  $P_0$  is set to  $0.5 \cdot I_5$ .

#### Following vehicle Kalman filter

The Kalman filter implemented in the following vehicles has the same model as the prediction model in the MPCs, and is discretized in the same manner using equations (3.39) and (3.40). The following vehicle Kalman filter has the identity matrix  $I_4$  as measurement matrix  $C$  and the covariance matrices contains the same values as the leading vehicle filter, expect for the curvature  $\kappa$  since its not included as a state. The initial guess  $P_0$  is set to  $0.5 \cdot I_4$ .

## 4.4 Modelling losses of lane marking detection

As noted in Chapter 1, the detection of the lane markings are not 100% reliable. For instance, sometimes gaps unexpectedly occur, e.g due to lane exits or a stand-still vehicle at the side. Seen in Figure 4.1 is an illustration of how the lateral offset could look like based on the lane markings if the right side has unreadable gaps. The red signal represents the lateral offset, i.e. distance to the middle of the lane. It is seen to be noisy close to zero at the straight road segment, then to have a spike. Going into the curve, the lateral offset is non-zero, and a spike occurs there as well. The last spike and the end of the curve are not shown in the road-illustration. These spikes are modelled to be one second in duration and thus correspond to losing the lane marking for 20 meters, given the vehicles speed of 20 m/s.

Log data received from Volvo show that each camera has a confidence value from 0-10, where 0 indicates a bad reading, and 10 indicates a very good reading. Right and left lane markings have separate confidence values, and in the scenario in Figure 4.1, only the right lane marking is unreliable, and the left could be relied on solely. The way losses of lane marking detection is modelled in this thesis does not take this redundancy into consideration. Even though it is rare that both lane markings become unreliable at the same time, this is the situations that this thesis does take into consideration.

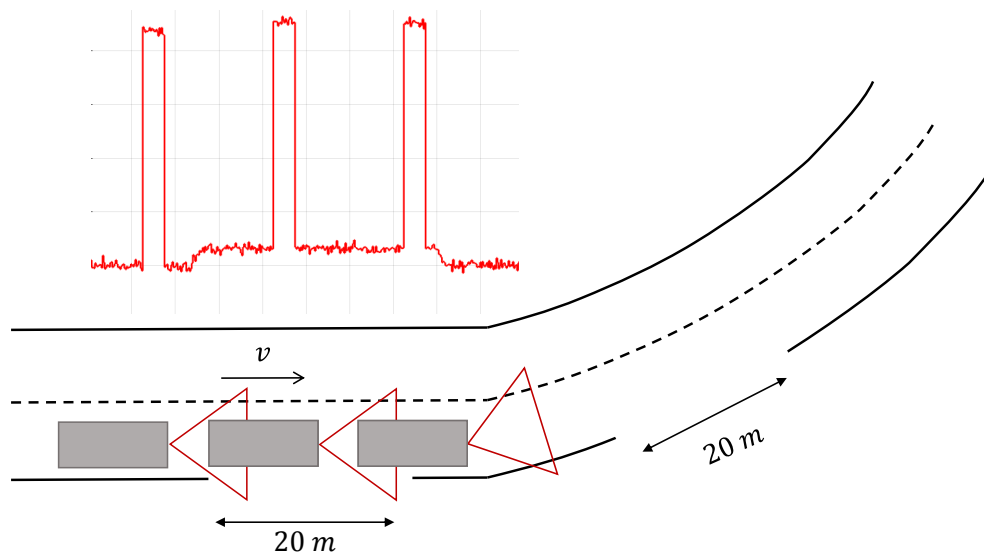


**Figure 4.1:** Illustration of what the distance to the center line  $y_{cl}$  looks like to the vehicle (red signal with spikes) in the events of lane marking losses (white spaces)

### 4.5 Simulation

The simulation and evaluation of the platoon using MPC has been carried out in PreScan. Figure 4.2 shows the evaluated platoon in the PreScan 3D environment. More information about PreScan can be read in section 4.5.2.



**Figure 4.2:** The evaluated platoon in PreScan environment with four HDVs with three following vehicles and one leading vehicle. The width of the lane is 3.5 meters and each HDV has a longitudinal speed of 20 m/s.

#### 4.5.1 Computer hardware specifications

The feasibility of the implemented MPCs in terms of computational demand is later to be discussed. The hardware specifications of the computer used for developing the MPC and of the computer used for running the simulation environment are

- Development computer
  - Windows 7 64-bit
  - Intel Core i5-3320M @ 2.6 GHz (4 CPUs)
  - 4 GB RAM
- Simulation computer
  - Windows 7 64-bit
  - Intel Xeon X5660 @ 2.8 GHz (6 CPUs)
  - 32 GB RAM

#### 4.5.2 PreScan

PreScan is a visual, Simulink-based simulation environment that has, among other features, models for roads, lane detection sensors and V2V communication. Some vehicle dynamic models are built in and it is possible to pass more detailed models through the Simulink interface. In other words, software-in-the-loop (SIL) and

model-in-the-loop (MIL) are supported. The inputs from PreScan to Simulink are sensor readings (including V2V communication) and vehicle states. As output from Simulink to PreScan, PreScan requires updated vehicle states. Typically a Simulink vehicle model is given a new steering angle or throttle/brake signal as input and the resulting updated states as output to PreScan. Experiment scenarios are built by placing road segments in a 2D scenario builder. Vehicles, with specified dynamics, are then placed on the roads, and sensors are connected to the vehicles. The sensors show up as Simulink blocks in the Simulink interface and pass the readings from the sensors as the simulation progresses. A 3D rendering of the vehicle on the 2D scenario is generated and visualized as the vehicles states are updated per sampling instant. A deeper description and use guide of PreScan can be found in [22].

### 4.5.3 Structure of implemented components and signal routing

The implementation of the platoon with the approach that each following vehicle tracks the leading vehicle described in 3.2.2 can be seen in Figure 4.3. As indicated, the leading vehicle transmits its current position through V2V to the first following vehicle, which will in turn transmit a waypoint at reference index  $i = 3$  (since there is a two sample delay) in its own reference trajectory just passed by the vehicle itself, to the second following vehicle. The pattern is repeatable, meaning that all the blocks are alike for each follower. If one more follower is to be added, a new instance of the reference generator block and MPC block can be used.

To account for sensor noise the reference data that is transmitted by the leading vehicle is first Kalman filtered. Each following vehicle has also one Kalman filter for its own internal states and camera measurements for the same purpose.

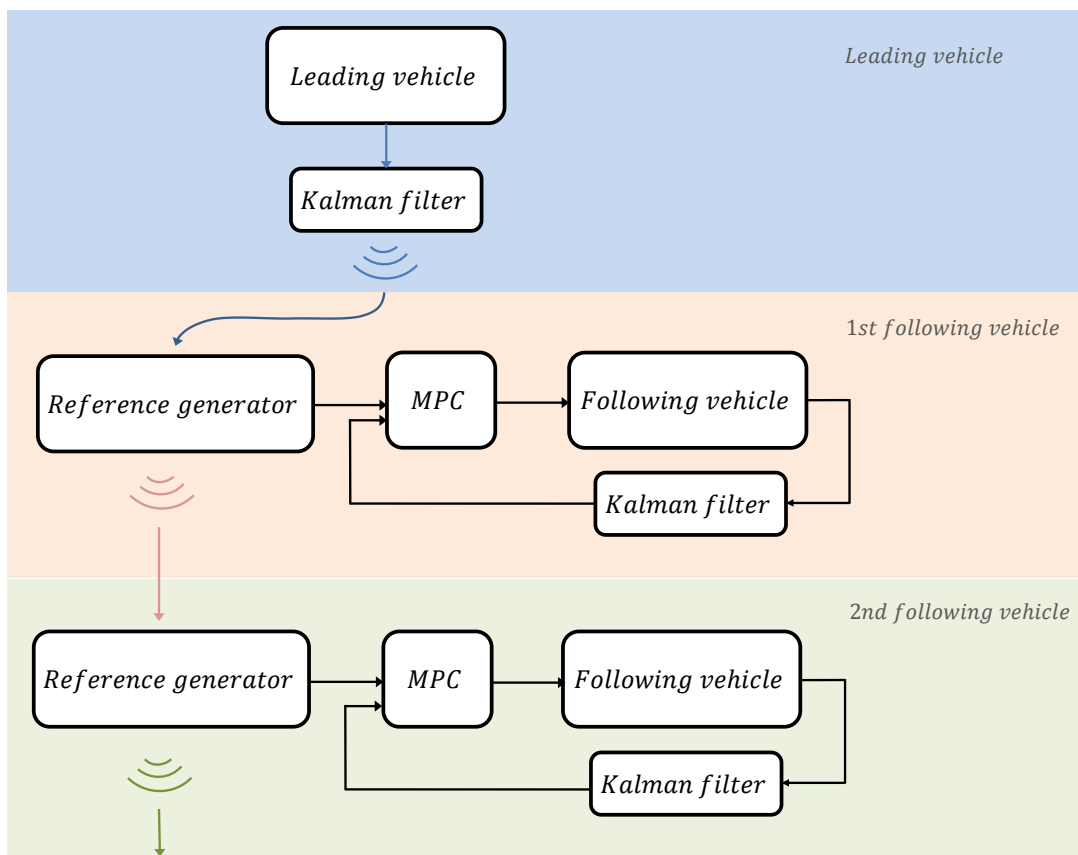


**Figure 4.3:** Implementation of the platoon in Simulink showing the structure and signal routing of the leading vehicle together with the two first following vehicles indicated with blue, red and green color respectively. This structure is based on the approach where each following vehicle tracks the leading vehicle, described in section 3.2.2.

# 5

## Results

In this chapter, results from simulating a platoon of four HDVs, including the leading vehicle, in PreScan are presented. All vehicles have separate but identical dynamics, namely a high fidelity HDV model provided by Volvo, and have local longitudinal velocities of  $20\text{ m/s}$ . Each following vehicle have a separate but identical MPC controller. The roads are flat and curves have a fixed radius of  $500\text{ m}$ . A transmission of information via V2V is modelled to have a delay of  $100\text{ ms}$ .

The considered simulation scenarios are

- Driving through a curve with a radius of 500 meters, seen in Figure 5.1.
- Avoiding an obstacle within its lane on a straight road, seen in Figure 5.2.

Furthermore, the figures in this chapter are shifted in time when several vehicles are shown, so that each value in the figures in the vertical direction corresponds to the same position on the road. This is done in order to be able to make an easier comparison.

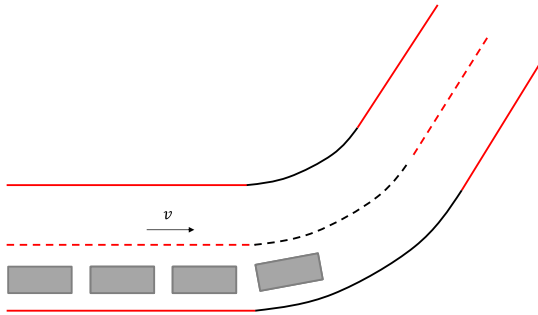


**Figure 5.1:** Simulation scenario when driving through a curve (black color) with a radius of 500 meters. The simulation starts and ends on a straight road segment, indicated by red color. For visualization purposes the curve is kept short in this figure but is longer in the actual simulation.

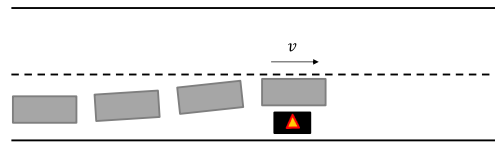


**Figure 5.2:** Simulation scenario when avoiding an obstacle within the lane on a straight road. The obstacle is indicated by the black box with a warning triangle and is assumed to be static.

### **5.1 Lateral control performance**

This section evaluates the behavior of the simulated platoon in absence of sensor noise, firstly using a local approach, i.e. that every vehicle only considers its directly preceding vehicle. The well known issue with maintaining string stability is seen. The preceding vehicle approach was then discarded due to the results shown below. Secondly, results using a global approach are presented, showing no propagation of errors.

#### **5.1.1 Reference tracking using preceding vehicle approach**

The reference tracking of the preceding vehicle approach have been evaluated with the two simulation scenarios described above. How the reference trajectories are generated using a preceding vehicle approach is described in Section 3.2.1.

### 5.1.1.1 Curve

The curvature of the simulated road can be seen in Figure 5.3 and the lateral offset  $y_{cl}$  and heading angle  $\Psi_{cl}$  can be seen in Figure 5.4 and Figure 5.5 respectively. It can be seen that the lateral offset to the middle of the lane is accumulating throughout the platoon members inside the curve, which is not desirable. Furthermore, the heading angle error accumulation of the vehicles in the platoon is not as significant when compared to the lateral offset.

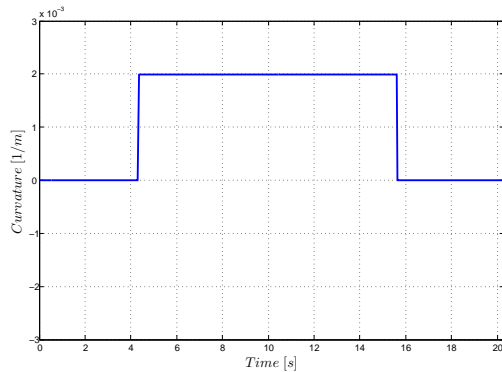


**Figure 5.3:** Curvature of the road as read perpendicular to the camera of the leading vehicle, through a curve with a radius 500  $m$ .

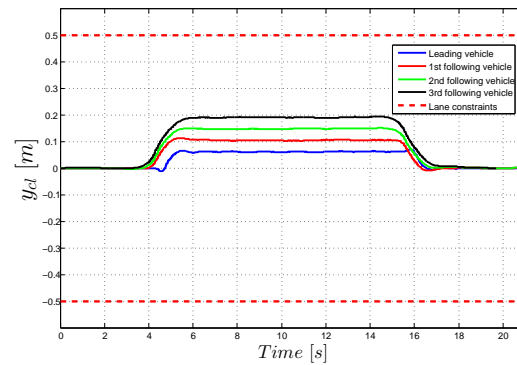


**Figure 5.4:** Lateral offset of the vehicles in the simulated platoon during a curve, using the preceding vehicle approach. As expected the errors accumulate, giving an increase of about 5 cm per vehicle.

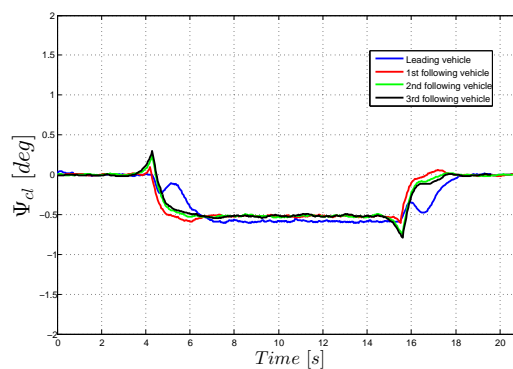


**Figure 5.5:** Heading offset of the vehicles in the simulated platoon during a curve, using the preceding vehicle approach. The heading error accumulation between the vehicles is not as significant.

### 5.1.1.2 Obstacle avoidance

The lateral offset and heading angle relative to the lane for all members of the simulated platoon can be seen in Figure 5.6 and Figure 5.7. The lateral offset of the following vehicles increases to the same value, although in the beginning of the manoeuvre the following vehicles further down in the platoon gets closer to the avoided object. Moreover, the heading angle of the following vehicles further down in the platoon gets smaller, which explains why the lateral offset gets closer to the avoided object.

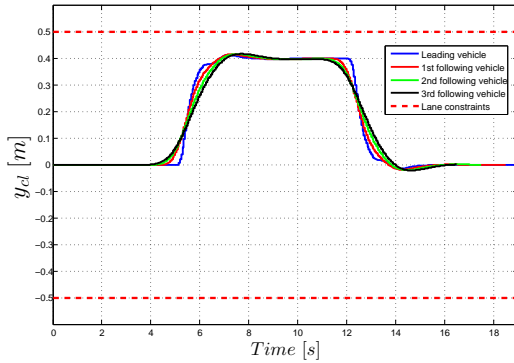


**Figure 5.6:** Lateral offset of the vehicles in the simulated platoon during an obstacle avoidance, using the preceding vehicle approach. Following vehicles get closer to the avoided object as they are further down in the platoon.

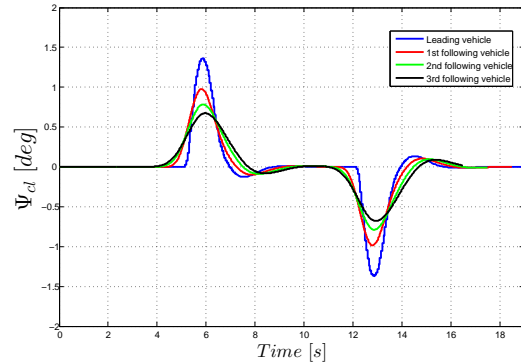


**Figure 5.7:** Heading offset of the vehicles in the simulated platoon during an obstacle avoidance. The change of heading gets less drastic for following vehicles further down in the platoon, which is not desirable when avoiding static obstacles.

## 5.1.2 Reference tracking using leading vehicle approach

The reference tracking of the leading vehicle approach have been evaluated with the same two simulation scenarios described above. How the reference trajectories are generated using a leading vehicle approach is described in section 3.2.2.

### 5.1.2.1 Curve

The curvature of the simulated road can be seen in Figure 5.3 and the lateral offset  $y_{cl}$  and heading angle  $\Psi_{cl}$  can be seen in Figure 5.9 and Figure 5.10 respectively. As seen in both the lateral offset and the heading angle, no accumulating errors throughout the platoon is present.

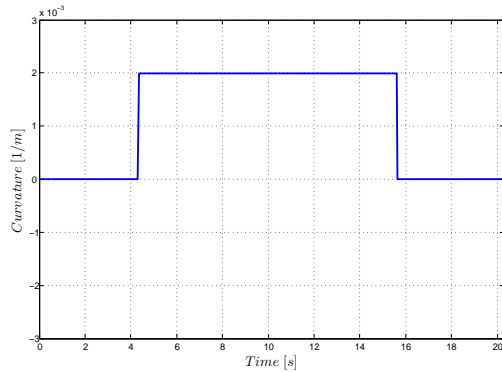


**Figure 5.8:** Curvature of the road as read perpendicular to the camera of the leading vehicle, through a curve with radius 500 m.

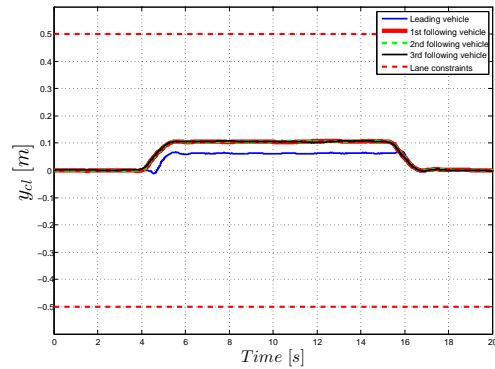


**Figure 5.9:** Lateral offset of the vehicles in the simulated platoon during a curve, using the leading vehicle approach. Following vehicles travels the same path with no accumulating errors.

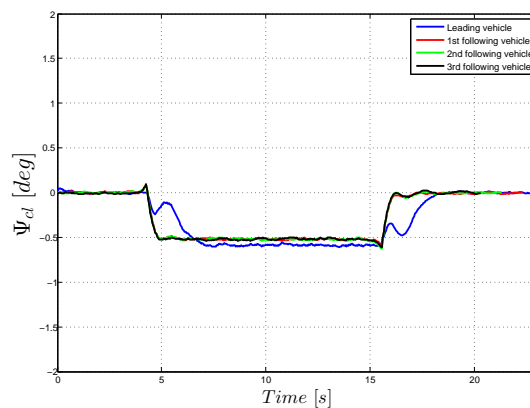


**Figure 5.10:** Heading offset of the vehicles in the simulated platoon during a curve. No heading error accumulation can be seen between the following vehicles.

### 5.1.2.2 Obstacle avoidance

The lateral offset and heading angle relative to the lane for all members of the simulated platoon can be seen in Figure 5.11 and Figure 5.12. It can be seen that no accumulating errors occur in the lateral offset and heading angle when avoiding an object in the lane.

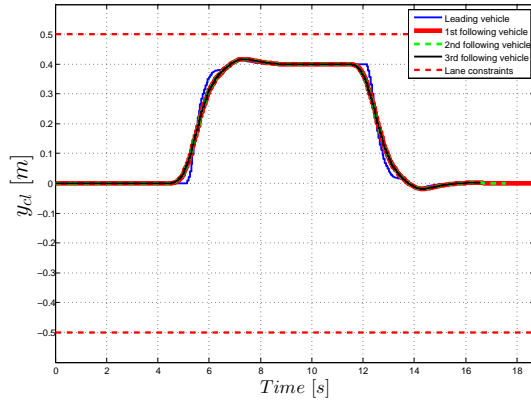


**Figure 5.11:** Lateral offset of the vehicles in the simulated platoon during an obstacle avoidance, using the leading vehicle approach. Following vehicles travels the same path during the obstacle avoidance.

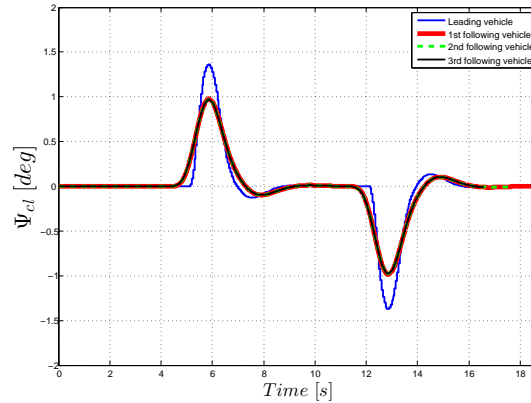


**Figure 5.12:** Heading offset of the vehicles in the simulated platoon during an obstacle avoidance, using the leading vehicle approach. The change of heading remains the same for all following vehicles further down in the platoon.

## 5.2 Ride comfort with and without preview information

This section shows how utilizing preview information propagated through V2V communication, coupled with the predictive nature of MPC, improve ride comfort. A common metric used to quantify ride comfort is the rate of change of acceleration, i.e. the derivative of acceleration w.r.t time, called jerk [23]. This section will show the steering wheel angle and the lateral jerk for a following vehicle and a leading vehicle when entering a curve and also when the leading vehicle avoids an obstacle on a straight road.

### 5.2.1 Curve

The steering wheel angle and lateral jerk for a following vehicle and the leading vehicle can be seen in Figure 5.13 and Figure 5.14 when driving through a curve. To show the effectiveness of the preview information of the future curvature, the leading vehicle has no knowledge of how the road looks ahead. In reality, the driver would naturally see how the road looks ahead and steer accordingly. However, this shows how the feed forward of the curvature to the following vehicle results in a more smooth steering and less lateral jerk.

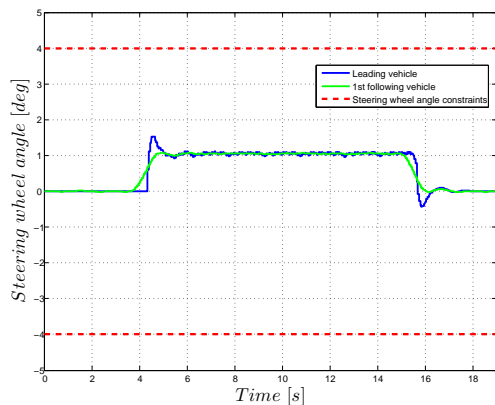


**Figure 5.13:** Steering wheel angles of a following vehicle driving through a curve with and without preview information of the road curvature. The steering wheel angle of the following vehicle with preview information is more smooth.

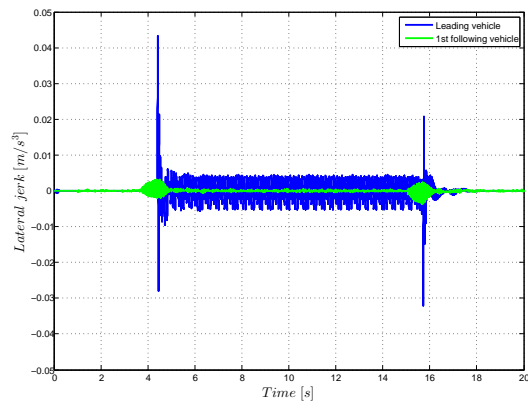


**Figure 5.14:** Lateral jerks of a following vehicle driving through a curve with and without preview information of the road curvature. The lateral jerk from the following vehicle with curvature preview has significantly less lateral jerk.

### 5.2.2 Obstacle avoidance

The worst case scenario when avoiding an obstacle in the lane is when it appears suddenly. That is the scenario that has been simulated. As expected, this causes a large amount of jerk for the leading vehicle which initiates the evasive manoeuvre. In Figure 5.15 it can be seen that the maximum required steering angle for the following vehicle is much lower than for the leading vehicle in order to avoid the object. Furthermore, in Figure 5.16 is how much smaller the lateral jerk is for a following vehicle that can adjust for the avoided object much earlier than the leading vehicle.

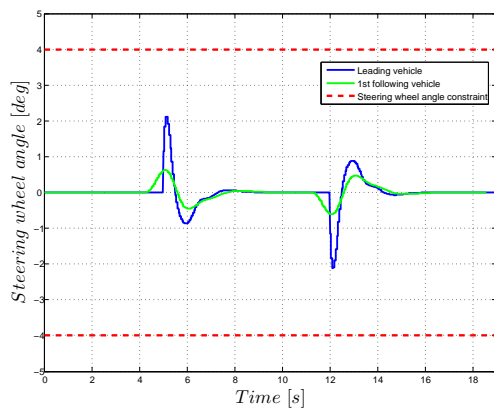


**Figure 5.15:** Steering wheel angles of a following and a leading vehicle during an obstacle avoidance manoeuvre on a straight road. The leading vehicle makes a sudden and harsh manoeuvre. The steering wheel angle of the following vehicle is more smooth due to the preview information of the leading vehicle's path.

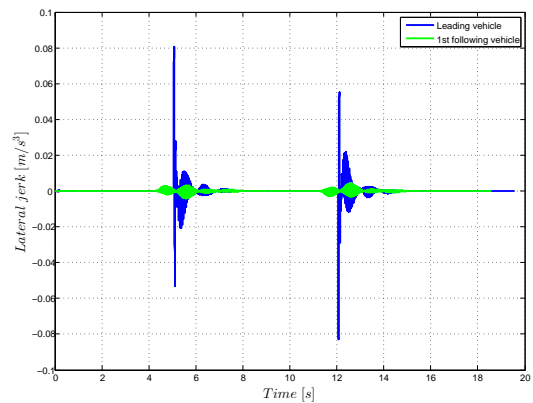


**Figure 5.16:** Lateral jerks of a following and a leading vehicle during an obstacle avoidance manoeuvre on a straight road. The leading vehicle makes a sudden and harsh manoeuvre. The lateral jerk of the following vehicle is significantly smaller due to the preview information of the leading vehicle's path.

### 5.3 Safety

A central appeal of an MPC control strategy is the possibility of implementing constraints. A road is naturally a constrained area. This section shows a way in which the following vehicles are protected, by use of constraints, from leaving the lane, even if the leading vehicle, unexpectedly, requests them to. One could note that certain situations might require leaving the lane for safety reasons, but these are not considered as stated in Chapter 1.

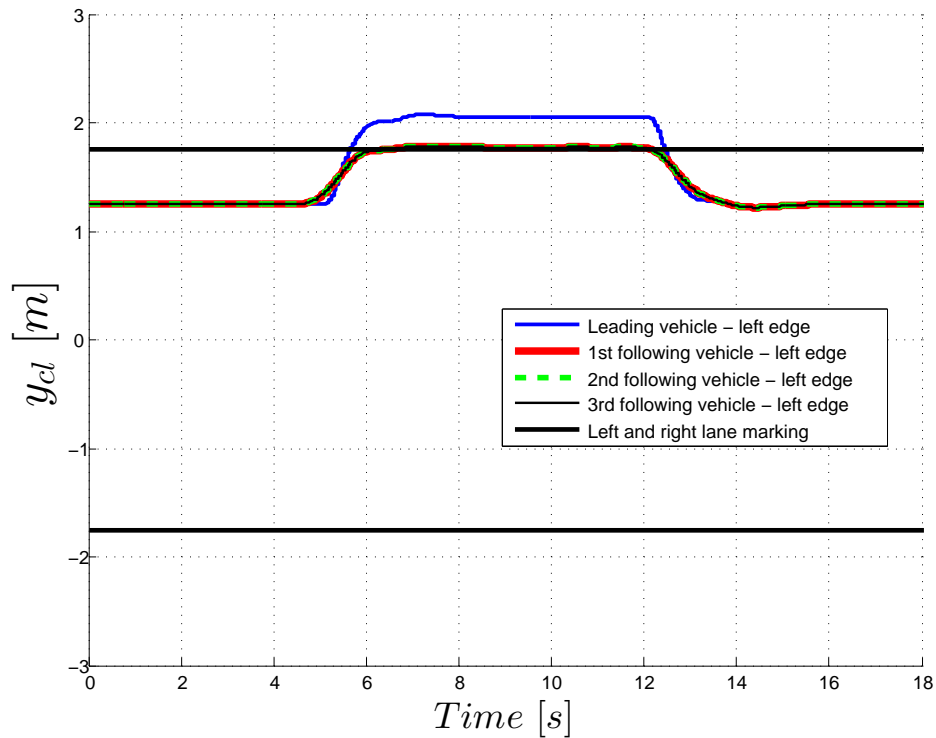


**Figure 5.17:** Reaction of the following vehicles when the leading vehicle unexpectedly maneuvers in such a way that the left out most edge exits the lane. The following vehicles stays within the lane.

## 5.4 Kalman filter performance

This section evaluates the filter performance in an open-loop simulation where each figure shows the true state, measured state and the filtered state. In the measured state, noise has been added manually. The Kalman filter in the following vehicles filters four states, as stated in Section 4.3. These states are  $\dot{y}$ ,  $\dot{\Psi}$ ,  $\Psi_{cl}$  and  $y_{cl}$ . In addition, the leading vehicle also filters the curvature  $\kappa$ . The added noise levels (standard deviation  $\sigma$ ) on the different states were estimated from real log data from a test track. Specifically, the standard deviation for the lateral offset measurements by the camera was obtained from a previous thesis [24]. Figures 5.18, 5.19, 5.20, 5.21, 5.22 and 5.23 shows the kalman filtered yawrate, lateral velocity, heading angle, curvature, lateral offset with noise and lateral offset with noise and sensor failures respectively. Worth to note is that the chosen curvature is difficult for a Kalman filter to capture, since it has very steep dynamics as seen in Figure 5.21. How the filtered curvature that grows slower than the actual curvature affects the rest of the system becomes apparent in later sections. Moreover, the filtered lateral offset in Figure 5.22 has a slight offset compared to the true lateral offset although capturing the same dynamics. Figure 5.22 shows how the Kalman filter copes with specific known sensor failures on the right lane marking. It does so by, during the failures, rely much less on measurements and much more on its prediction model.

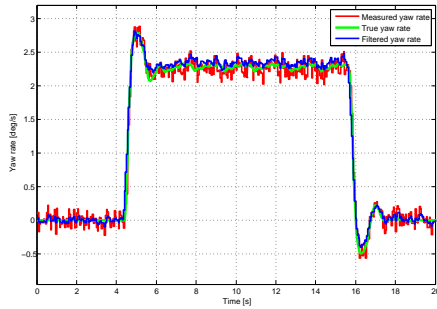


**Figure 5.18:** True, measured and filtered yaw rate.

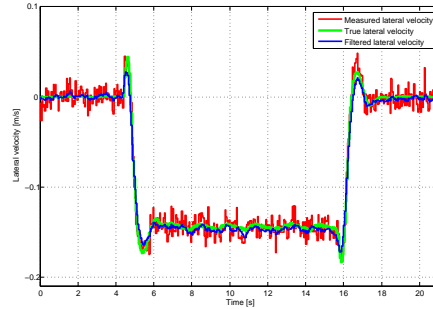


**Figure 5.19:** True, measured and filtered lateral velocity.

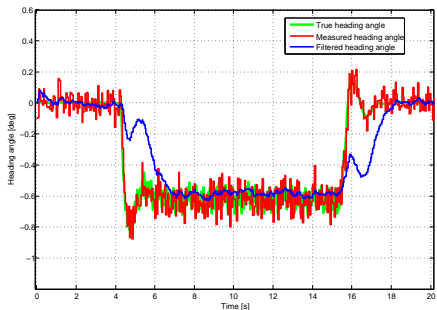


**Figure 5.20:** True, measured and filtered heading angle  $\Psi_{cl}$ .

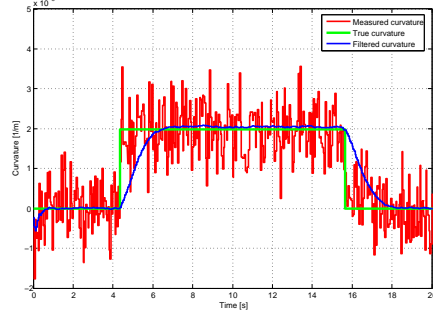


**Figure 5.21:** True, measured and filtered curvature  $\kappa$ .

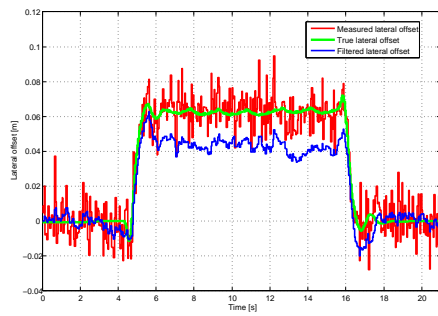


**Figure 5.22:** True, measured and filtered lateral offset  $y_{cl}$  in absence of sensor failures.

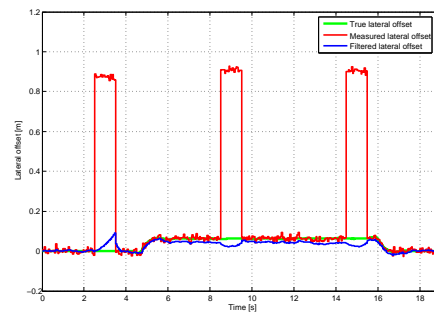


**Figure 5.23:** True, measured and filtered lateral offset  $y_{cl}$  in presence of specific sensor failures added on the right lane marking.

## 5.5 Lateral control performance with added noise

Effects of Kalman filtering when going through a curve are seen comparing Figure 5.24 and Figure 5.25 below. The comparison is between not filtering the references from the leading vehicles and not filtering the measurements taken by the following vehicles versus filtering both. The filtered case shows two bumps in lateral offset when entering and leaving the curve, explained by Figure 5.21, which shows that the filter makes it seem like the curvature is coming gradually instead of stepwise, as it actually is. Furthermore, seen in Figure 5.26 and Figure 5.27 is how the filter significantly reduces changes in steering wheel angle and lateral jerk. It can also be seen that the filtered steer wheel angle in Figure 5.26 increases slightly later when entering (and leaving) the curve than the unfiltered signal. This is because of the way the curvature  $\kappa$  is filtered as shown in 5.21.

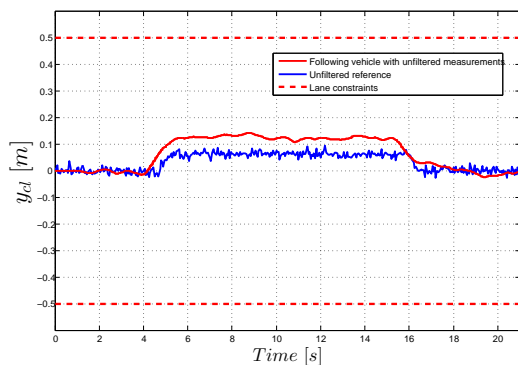


**Figure 5.24:** Lateral offset in a curve with unfiltered references from the leading vehicle and unfiltered measurements from the following vehicle's sensors.

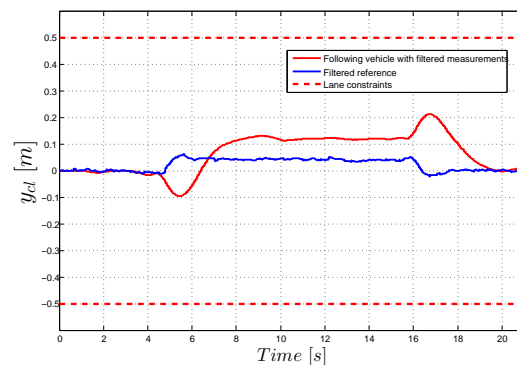


**Figure 5.25:** Lateral offset in a curve with filtered references from the leading vehicle and filtered measurements from the following vehicle's sensors.

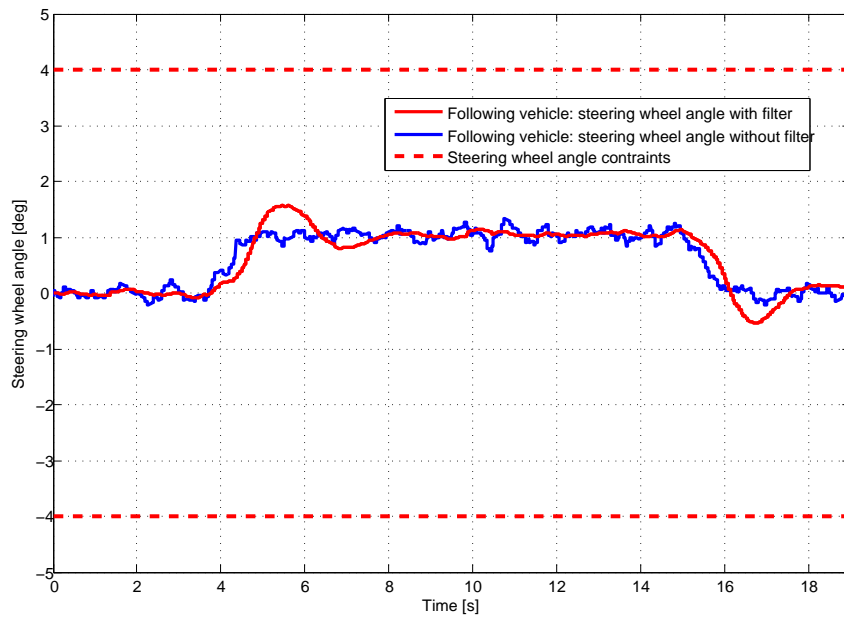


**Figure 5.26:** Steering wheel angles of a following vehicle in a curve for the unfiltered and filtered case. The steering wheel angle for the filtered case is more smooth.

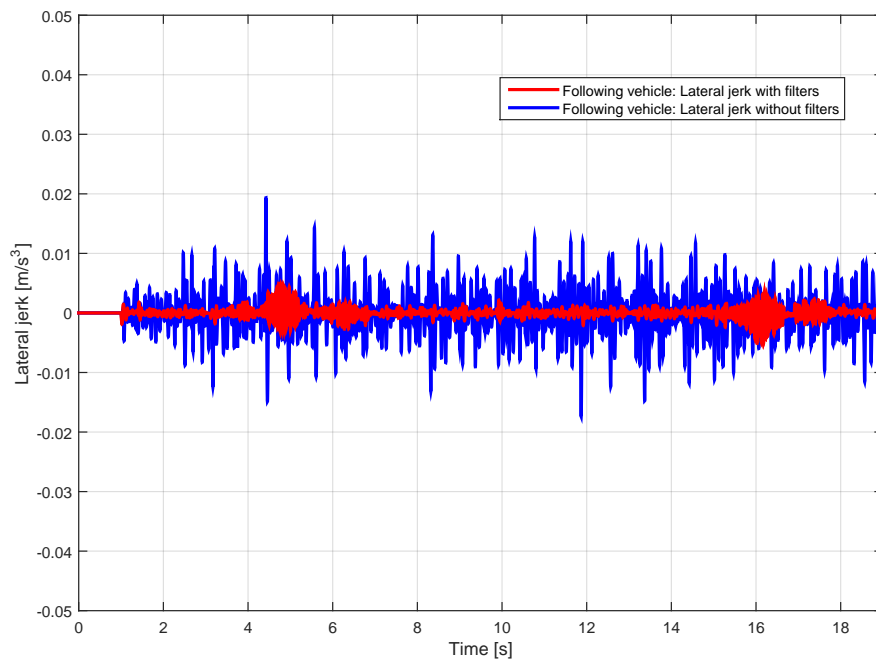


**Figure 5.27:** Lateral jerks of a following vehicle in a curve for the unfiltered and filtered case. Significantly less lateral jerk for the filtered case.

## 5.6 Lateral control performance with added noise and sensor failures

In addition to adding sensor noise, sensor failures are also added on the lateral offset measurements. A comparison between not filtering sensor failures in the reference and in the following vehicle versus filter both are seen in Figures 5.28 and 5.29. As expected, not filtering failures on neither the reference nor following vehicle is catastrophic. Filtering both reference and following vehicle shows vast improvement. Figure 5.30 show the steering wheel angle for the filtered and unfiltered case, and Figure 5.31 show the lateral jerk for the filtered and unfiltered case.

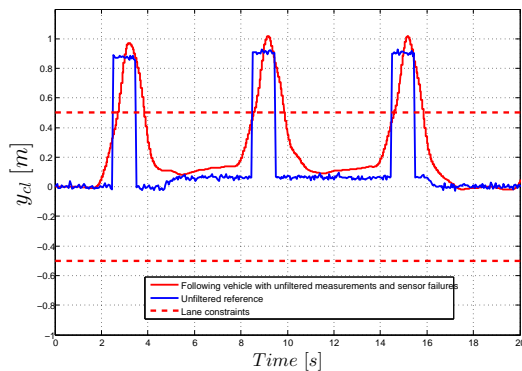


**Figure 5.28:** Lateral offset in a curve with unfiltered references from the leading vehicle and unfiltered measurements from the following vehicle's sensors. Additionally, sensor failures are added on the lateral offset in both the leading vehicle's reference and on the following vehicle's own measurements.

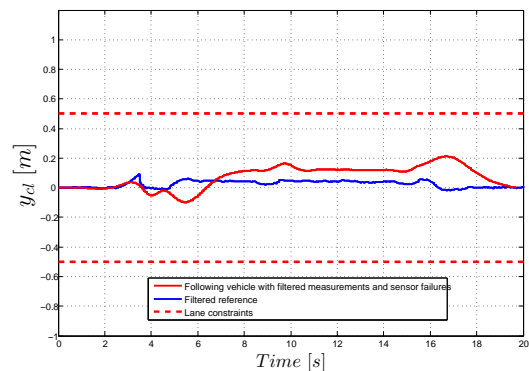


**Figure 5.29:** Lateral offset in a curve with filtered references from the leading vehicle and filtered measurements from the following vehicle's sensors in presence of sensor failures on both the leading vehicle's reference and on the following vehicle's own measurements.

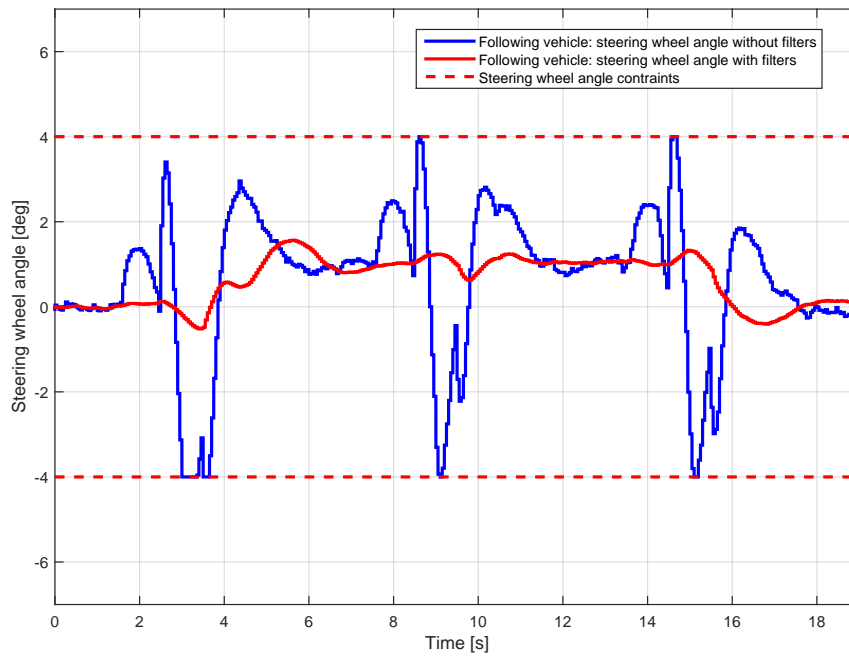


**Figure 5.30:** Steering wheel angles of a following vehicle in a curve for the unfiltered and filtered case in presence of both noise and sensor failures. It can be seen that the constraints for the unfiltered case gets activated several times.

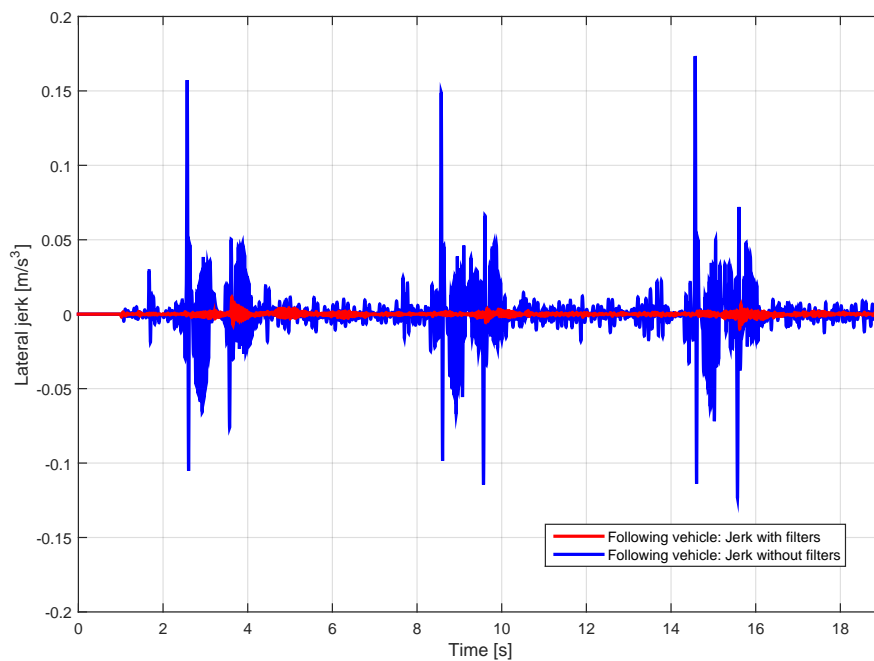


**Figure 5.31:** Lateral jerks of a following vehicle in a curve for the unfiltered and filtered case. Again, significantly less lateral jerk for the filtered case.

## 5.7 Computation time

Solving one MPC optimization yielding the next control input as described by equations (4a-h) with prediction model as described by equation 3.23 on the simulation computer with hardware specifications as described in Section 4.5.1 took about 1.6 milliseconds. On the development computer with specifications described in the same section, it took about 3.8 milliseconds.



# 6

## Discussion

This chapter provides a discussion about the reference generation and about the results. Additionally, a brief discussion about real life viability and non-linear MPC is given in the end of the chapter.

### Reference generation

In the leading vehicle approach a decision was made to let the reference trajectories from the leading vehicle pass through each following vehicle instead of passing it directly from the leading vehicle to the each follower. As far as the authors of this thesis sees it, there is a trade off between longer vision versus computation time, modularity and memory usage. Either one could increase the horizon length for each following vehicle further down in the platoon so that all vehicles reaches the leading vehicles camera, or keep the horizon length constant as it is implemented in the leading vehicle approach, but then store the values in a buffer before it is used. If increasing the horizon length, the computation time and memory usage would increase for each MPC further down in the platoon, yet it is also unclear how much benefit an increased horizon would give, since the model mismatch between the prediction model in the MPCs would increase if the horizon is longer, and might result in a less accurate control signal. Having different horizon lengths would lead to loss of modularity which means that a different setup needs to be implemented depending on which position a vehicle has in the platoon. In case of the other approach where the horizon length is kept the same for all vehicles but the references are stored in a buffer, this would also require a different reference generator setup depending on the position on a vehicle in the platoon. In the leading vehicle approach in this thesis, the modularity is kept and the approach requires less computational time and memory usage compared to a increasing horizon approach which is important when implementing in real HDVs.

### Lateral control performance without noise

The preceding vehicle approach caused accumulating errors as expected. Even though these errors are not increasing rapidly, due to the performance of the MPC, they are not desirable. The leading vehicle approach did not cause accumulating errors which was also expected. However, one drawback with the leading vehicle approach is the accuracy for vehicles in the further down in the platoon when considering measurements of the longitudinal distance, as they need to dead-reckon

their travelled distance for a long time. This thesis assumed a constant longitudinal velocity. In a real life implementation, how viable the leading vehicle approach is thus seems to rely much on the reliability of the estimated longitudinal speed. The distance between the vehicles can be assumed to be well known due to the accuracy of the radar. The lengths of each vehicle in the platoon seem reasonable to share via the V2V communication which motivates the assumption that the length between the vehicles in the platoon are known. Moving on, another challenge might be the reliability of the V2V communication. This thesis assumed a constant and known V2V delay. The effects of a varying and unknown delays are hard to predict.

### **Ride comfort**

When choosing control strategy, a global approach with MPC was chosen. The reasoning behind it was that one could utilize the predictive nature of MPC together with the look-ahead information shared via V2V communication. It did, as reasoned, turn out to have a noticeable positive effect on the smoothness of steering and thereby ride comfort both in curves and when avoiding objects, compared to a look-down approach. Although the comparison was performed with a leading vehicle without preview and a following vehicle with preview the comparison could just as well have been performed between two following vehicles, one without and one with preview.

### **Safety**

The constraints that limits the HDVs from leaving the lane performed as intended, even when the HDVs was requested to leave the lane. As it can conceivably be dangerous to be "trapped" in the lane, additional control logic needs to be implemented about when these constraints should be active or not. This, however, is on a higher decision level then the developed controller, and could e.g best be implemented by letting the leading vehicle driver make those decisions. The safety chapter was presented to show the possibilities when using MPC in platooning.

### **Kalman filter performance**

Noise caused a vast reduction in ride comfort. The Kalman filters however reduced this reduction considerably. The added noise on each signal seem realistic, since the standard deviations are estimated from real log data on a test track. However, on real roads the data would most likely not look as pretty as from the log data on the test track with possibly higher noise levels. Though adding these noise levels is a step towards reality. Furthermore, the filtering of the lateral offset has an offset which possibly is due to a model mismatch between the Kalman process model and the actual true lateral offset. Additionally, the curvature in the simulation tests was chosen to change instantly between zero and the curvature value in order to showcase the 'worst' scenario. These kinds of non-dynamic changes seem hard to model with

a linear Kalman filter if one would want to remove most of the noise levels as seen in Figure 5.21, where the filtered curvature increases slower. In reality, the curvature is not changing as rapidly and would make it easier to filter. In this thesis sensor failures was only considered on the lateral offset measurements. Additional steps would be to add sensor failures also on the measured curvature and heading angle which will appear in reality. Also, sensor failures might not be as easily detectable as stated in Chapter 1. This would require an improved filter.

## Lateral control performance with added noise

Unfiltered noisy signals did not cause an unstable platoon, however it decreased ride comfort significantly. The reason noise did not cause too violent steering may have to do with the fact that both  $\Delta u$  and  $\Delta^2 u$  are weighted and constrained. The weights certainly kept the steer wheel velocity and acceleration down, acting as a sort of inertia or low pass filter and not letting the high frequency components of the noise affect the HDVs too much.

## Lateral control performance with added noise and sensor failures

The sensor failures were modelled as one second windows where the distance to the lane centerline was given bogus values. These were handled by tuning the Kalman filter to rely much more on the model than the measurements while the failure was occurring (i.e. the measurements were known to be of bad quality when they occurred). The Kalman filter made the sensor failures to only have centimeter-effects on the lateral offset, even in curves. It is hard to know what is deemed good or bad filter performance on sensor failures. Given the length of the simulated failures and that they are treated as if both left and right lane markings are unreliable, which they probably are not very often, the filter seems efficient, even in curves. The bogus values were added on the right lane marking. How the filter handles bogus values on the left lane marking is yet to be considered, although these kinds of failures seem to occur most often on the right lane marking, as seen in Figure 1.1.

## Computation time and real life viability

The MPCs are set to run once every 50 milliseconds and thus gives new steering angles to the vehicles. On the simulation computer, with specifications listed in Section 4.5.1, one MPC execution took about 1.6 milliseconds corresponding to 3.2% of the sample time of the MPC. On the development computer, it took about 3.8 milliseconds corresponding to 7.8% of the sample time. The dSpace Autoboxes often used with Rapid Control Prototyping (RCP) for testing in prototype vehicles are however significantly much more constrained in hardware. Comparing the performance of a dSpace Autobox with the computers used to develop and simulate the MPC and Kalman filters seems difficult and is left for future work.

## **Linear versus non-linear MPC**

Increasing the accuracy of the prediction model even more could be achieved by using a non-linear prediction model instead of a linear one. This however would require a linearization at each sampling instant, which means an increase in computational demand. Conversely, if the linear prediction model turns out to be too computationally demanding itself, one could look into an explicit MPC which, thanks to the linearity, uses precomputed solutions instead of run-time optimization.

# 7

## Conclusion

Driving in a platoon on highways have many benefits, although this give rise to technical challenges which needs to be tackled in order for platooning to become reality. The objectives of this thesis were to investigate some of these challenges, more specifically, the objectives of this thesis were to

- identify which sensor information and V2V communication is needed to generate reference signals to a lateral control system
- decide what control strategy is suitable for this application
- design, implement and evaluate the control system in a simulation environment
- be able to handle specific sensor failures

The developed MPC and Kalman filters meet the objectives set for this thesis. Combining the selected sensors and V2V communication provides the lateral control system with sufficient information for the tested scenarios. The MPC handles the steering automatically and thus enables smaller longitudinal distances between vehicles in platooning. No real drawback is noted with this approach, except potentially the computational demand and memory usage when implementing in real vehicles.



# 8

## Future Work

There are a lot interesting work that has been discovered while conducting this thesis. Relevant future work which is of particular interest are listed here.

### **Varying inter-vehicular distance**

It would be preferred to have varying inter-vehicular distance, especially given hills, where CACC systems would want a varying distance for fuel-saving purposes. The remedy is not very complex though, as the distance and longitudinal velocity can be read at each sampling instant, giving the required time gap, which is then divided by the number of prediction steps giving the required sampling time. The prediction model is then re-discretized with this sampling time giving a longer or shorter prediction horizon depending on the current time gap.

### **Improving the perception part**

This thesis showed that having a filter which can handle sensor failures is necessary. The implemented linear Kalman filters shows improvement in ride comfort and keeps the vehicle reasonably stable even when its "blind" regarding the distance to its lane markings for relatively long periods of time. However, much more work could go into this, where additional sensor failures on other measurements can be added and also failures which are less detectable in the sense that it does not give a very low confidence value on the measurements which have been assumed in this work.

### **Varying longitudinal speed**

The longitudinal speed was assumed to be constant at 20 m/s, i.e. 72 km/h. The longitudinal speed effects the lateral dynamics of the prediction model in the MPCs. A linear time-varying (LPV) model instead of a strictly linear model could be used pretty easily. A look-up table of tuning parameters for different longitudinal speeds is then needed.

### **Modelling packet losses and varying delays**

The V2V communication used in this thesis is well-behaved. How much different percentages of packet losses affects performance can be investigated as well as the effect of varying delays.

### **Turning lane constraints on/off**

As discussed in the report, restricting the vehicles in the platoon to the lane in focus is both good and potentially bad. The constraints of the lateral offset need to be possible to turn off, either as a separate feature or as a part of instantly dissolving the platoon, or both.

### **Constraining steering wheel angle acceleration**

Constraining and weighting the steering wheels angular velocity  $\Delta u$  improved the performance of the MPC significantly, and thus the decision to constrain and weight the steering wheel acceleration  $\Delta^2 u$  was made. Though,  $\Delta^2 u$  did not hit its constraints practically at any time, even though its weight likely made the steering smoother. Further testing constraining the steering wheel acceleration is recommended.

### **Different sample times**

The choice of sample time was not evaluated against other sample times. This is interesting to look into, seeing how much lower or higher one can go, and the benefits and drawbacks of both cases.

### **Evaluate code efficiency**

In order to be tested in a dSpace Autobox, the developed algorithms most likely need to be written more efficiently w.r.t. memory usage and processor usage.

# Bibliography

- [1] ACEA. *Trucks, Vans, Buses*. <http://www.acea.be/automobile-industry/trucks-vans-buses>.
- [2] Scania. *Annual report 2001*. [http://www.scania.com/group/en/wp-content/uploads/sites/2/2015/09/sca01EN\\_tcm10-8527\\_tcm40-543841.pdf](http://www.scania.com/group/en/wp-content/uploads/sites/2/2015/09/sca01EN_tcm10-8527_tcm40-543841.pdf). 2002.
- [3] Scania. *Platooning saves up to 12 percent fuel*. <http://www.scania.com/group/en/platooning-saves-up-to-12-percent-fuel>. 2015.
- [4] Sadayuki Tsugawa, Shin Kato, and Keiji Aoki. “An Automated Truck Platoon for Energy Saving”. In: *2011 IEEE/RSJ International Conference on Intelligent Robots and Systems. San Francisco, CA, USA*. 2011.
- [5] Sadayuki Tsugawa. “Final Report on an Automated Truck Platoon within Energy ITS Project”. In: *International Task Force on Vehicle Highway Automation 17th Annual Meeting*. 2013.
- [6] Fred Browand and Mark Michaelian. “Platoon Travel Saves Fuel. . . How Much?”. In: *Research Updates in Intelligent Transportation Systems Volume 9 No. 2*. 2000.
- [7] Michael P. Lammert et al. In: *SAE Int. J. Commer. Veh.* 7(2):2014, doi:10.4271/2014-01-2438.
- [8] Stefan Solyom, Arash Idelchi, and Badr Bin Salamah. “Lateral Control of Vehicle Platoons”. In: *IEEE International Conference on Systems, Man, and Cybernetics*. 2013.
- [9] Günter C. Keßler, Mathias Hakenberg, and Stefan Deutsche Dirk Abel. “Lateral Control of Heavy-Duty Vehicle Platoons Using Model-Based Predictive Control”. In: *6th IFAC Symposium Advances in Automotive Control Munich, Germany, July 12-14*. 2010.
- [10] Jano Yazbeck et al. “Decentralized local approach for lateral control of platoons”. In: *INRIA, September 2010*, [http:// hal.inria.fr/inria-00547567/en.Other\\_Publications](http://hal.inria.fr/inria-00547567/en.Other_Publications).

- [11] Papadimitriou, I. and Tomizuka, M. (2004) 'Lateral control of platoons of vehicles on highways: the autonomous following based approach', *Int. J. Vehicle Design*, Vol. 36, No. 1, pp.24-37.
- [12] Arash Idelchi and Badr Bin Salamah. "Lateral Control of Vehicle Platoons". MA thesis. Gothenburg: Chalmers University of Technology, 2011.
- [13] Sugimachi, Toshiyuki; Fukao, Takanori; Yoshida, Jun et al. 'Autonomous Driving Based on LQ Path Following Control and Platooning with Front and Rear Information', *17th ITS World Congress, Busan, 2010: Proceedings (2010): 12p.*
- [14] Roozbeh Kianfar, Paolo Falcone, and Jonas Fredriksson. "A Distributed Model Predictive Control Approach to Active Steering Control of String Stable Cooperative Vehicle Platoon". In: *7th IFAC Symposium on Advances in Automotive Control. The International Federation of Automatic Control September 4-7. Tokyo, Japan.* 2013.
- [15] Simo Särkkä. *BAYESIAN FILTERING AND SMOOTHING*. Cambridge University Press, 2003.
- [16] J Förstberg M Balli G Lauriks J Evans and I Barron de Angoiti. *Swedish National Road And Transport Institute : UIC comfort tests - Investigation of ride comfort and comfort disturbance on transition and circular curves.* 2003.
- [17] Rajesh Rajamani. *Vehicle Dynamics and Control*. Springer, 2005.
- [18] Stéphanie Lefèvre, Yiqi Gao, Dizan Vasquez, H. Eric Tseng, Ruzena Bajcsy, et al.. Lane Keeping Assistance with Learning-Based Driver Model and Model Predictive Control. 12th International Symposium on Advanced Vehicle Control, 2014, Tokyo, Japan.<hal-01104458>.
- [19] Valerio Turri et al. *Linear Model Predictive Control for Lane Keeping and Obstacle Avoidance on Low Curvature Roads.* 2013.
- [20] Roozbeh Kianfar et al. *Combined Longitudinal and Lateral Control Design for String Stable Vehicle Platooning within a Designated Lane.* 2014.
- [21] Alexander Domahidi and Juan Jerez. *FORCES Professional*. <http://embotech.com/FORCES-Pro>. 2014.
- [22] Magnus Almroth. "Simulation, validation and design of cooperative driving systems using PreScan". MA thesis. Stockholm: KTH Royal Institute of Technology, 2013.

- [23] G Lauriks et al. *Swedish National Road And Transport Institute : UIC comfort tests - Investigation of ride comfort and comfort disturbance on transition and circular curves*. 2003.
- [24] Arni Thorvaldsson Vinzenz Bandi. “Reference Path Estimation for Lateral Vehicle Control”. MA thesis. Gothenburg: Chalmers University of Technology, 2015.